Stem cell derived neurons: Physiology of early differentiation and development

Inauguraldissertation

zur

Erlangung der Würde eines Doktors der Philosophie

vorgelegt der

Philosophisch-Naturwissenschaftlichen Fakultät

der Universität Basel

von

Lydia Barth

aus Gera, Deutschland

Basel 2015

Genehmigt von der Philosophisch-Naturwissenschaftlichen Fakultät
auf Antrag von:

Fakultätsverantwortlicher:	Prof. Dr. Kaspar Vogt
Korreferent:	Prof. Dr. Heinrich Reichert

Basel, 17.09.2013

Prof. Dr. Jörg Schibler
Dekan

„Unsere grösste Schwäche liegt im Aufgeben. Der sicherste Weg zum Erfolg ist immer, es doch noch einmal zu versuchen.“ (Thomas Alva Edison)

Contents

Summary

The developing nervous system of vertebrates is largely inaccessible; especially early neuronal differentiation and development are difficult to study. Early events in neurogenesis can be investigated more easily by using murine embryonic stem (mES) cells. Under suitable culture conditions mES cells pass through all phases of neural differentiation through an intermediate stage of embryoid bodies. As wild type or genetically modified ES cells can be grown in unlimited quantities, their differentiation into neurons represents an attractive model for studying neurodevelopmental diseases. Functional neuronal maturation can now be followed from immature to mature neurons forming excitatory and inhibitory synaptically connected networks.

In my thesis work I used such a culture system to compare the functional development of mES cell derived neurons from different genetic backgrounds. I spent a lot of time establishing experimental conditions to study these cells using electrophysiological techniques. I quantified several key parameters such as resting membrane potential, voltage-gated channel activity, appearance of action potentials, to describe the neuronal differentiation of the cells. In the first days after seeding the precursors possess an immature physiology, with high input resistances, few voltage-sensitive conductance and immature spiking patterns. During subsequent development an increasing amount of voltage gated sodium- and potassium currents appeared, leading to more and more mature spiking patterns. Mature neurons form synaptically connected networks containing excitatory and inhibitory neurons. We investigated the development of spontaneous excitatory- and inhibitory postsynaptic currents (sEPSCs and sIPSCs) in these cultures.

We then built upon this knowledge of normal development to study mES cell-derived neurons defective in MeCP2 signaling. This genetic defect causes an important neurodevelopmental defect in mice and in humans. We were able to show that key features of the developmental defect – a disturbed maturation of inhibitory synapses – could be reproduced in our system. For further characterization of inhibitory interneurons we derived stem cells from a GAD67-GFP cell line under two pharmacological conditions as KCl and TTX which change the activity level up or down. This will aid to understand more about the developmental processes of neurons and will help finding functional deficits in neurodevelopmental diseases.

I. Introduction

Already 2500 years ago the famous Greek physician Hippocrates discovered the brain as the center of intelligence and sentience. Many years later the neuroanatomist Santiago Ramon y Cajal described the brain as a complex network of individual neurons. Ever since the architecture of the brain and the mechanisms guiding its neuronal assembly are being intensely studied.

The nervous system can be divided into two main parts, the central nervous system (CNS) containing the brain and the spinal cord. Its main job is to get information from the body and send out instructions. The peripheral nervous system (PNS) is made up of all the nerve cells outside of the CNS and their axons and its task is to sense the environment and the inner state of the body and to translate the instructions from the CNS into actions. This complexity and specialization makes it a unique system in the body to convey information to many different places, sometimes to multiple locations and over long distances in a very short time. Therefore, nerve cells form functional circuits that help to solve specific problems like feature detection on the sensory side e.g. vision, hearing or patterning of different types of movements such as locomotion, respiration and saccadic eye movements. Processing so many kinds of information requires many specialized neurons - there may be as many as 10,000 different types. The brain itself consists of around 200 billion neurons. Each of these neurons is connected to between 5,000 and 200,000 other neurons.

Neurons have many different shapes and sizes. A typical neuron has four defined parts: the cell body, dendrites, the axon and synaptic terminals. The cell body is contains the nucleus, mitochondria and other organelles. Dendrites transmit electrical signals to the cell body and receive signals from other neurons. The axon conducts information away from the cell body.

A neuron may have many dendrites, but it will have only one axon. One single neuron can be in contact with thousands of other neurons through synapses. Synapses are the junctions for communication. Neurons are located at different regions in the brain thus dendritic trees, axon branching and number of synaptic terminals depend on the neuron’s location. For example motor neurons need to have a more complex dendritic tree than sensory neurons because the reflex activity requires many excitatory and inhibitory neurons.

The rapid signaling in the CNS depends on ion channels, which can be ligand gated or voltage-dependent. Ligand gated channels mediate synaptic signals, whereas voltage-dependent ion channels produce intrinsic electrical signals, such as action potentials. Voltage-dependent ion channels (VDICs) are composed of several subunits with a central pore through which the ions (e.g. Na^+, K^+ and Ca^{2+}) move down their electrochemical gradient and are activated by changes in electrical potential difference near the channel. VDICs enable various characteristics of intrinsic neuronal excitability through which the neurons are able to display a fullness of firing behaviors over a wide range of stimuli and firing frequencies. Voltage-gated calcium channels play a role in neurotransmitter release in presynaptic endings and can control the shape of action potentials (APs) generated by Na^+ conductance changes. Voltage-gated sodium channels can be found in three different stages: deactivated (closed), activated (open), or inactivated (closed). Typical for most voltage-gated sodium channels is their property to inactivate within milliseconds. Voltage-gated potassium channels play an important role during APs by returning the depolarized cell to a resting state and are typically slow and non-inactivating. All the mentioned properties of the voltage-gated channels have an influence on the duration and rate of AP firing with crucial implications for axonal conduction and synaptic transmission. The expression of ion channels and their physiological properties are modulated and involved during cell differentiation (Ribera 1999), (Spitzer, Vincent et al. 2000).

The coordinated opening of voltage-gated Na^+ and K^+ channels generates the action potential and sends the electrical signal down the axon. APs occur in an all-or-none fashion after the neuron has reached a certain threshold. After the neuron has fired, there is a refractory period in which another action potential is not possible. During this time, the potassium channels reopen and the sodium channels close and the neuron returns to its resting membrane potential (RMP).The RMP is the membrane potential of a cell at rest, which results from the separation of positive and negative charges across the cell membrane and it averages -60 mV. It is made up of the equilibrium potential of all involved ions (Na^+: +60 mV, Cl^-: -70 mV, K^+: -80 mV) and is close to the potassium equilibrium potential.

Another feature of neurons is that they are connected with each other over a network where a signal is transmitted from one neuron to another through an electrical or chemical synapse. At electrical synapses two neurons are physically connected to each other via gap junctions. A chemical synapse is formed between the axonal terminal of one neuron and the postsynaptic specialization on the dendrites of another neuron and uses chemical signals to transmit information. After an electrical signal has travelled along an axon to the synapse, it causes the release of neurotransmitters. The most important neurotransmitters in the brain are acetylcholine, glutamate, GABA and dopamine. Specific receptors for the neurotransmitter are clustered at the surface of the receiving cell; these produce an electrical signal upon binding of the transmitter. The nerve cell transmitting a signal is called the presynaptic cell; the cell receiving the signal is the postsynaptic cell.

The change in membrane potential resulting from the receptor opening is called postsynaptic potential (PSP). Depending on which transmitter the synapse is releasing and which receptors are activated by this process, the effect can be excitatory (EPSP) or inhibitory (IPSP). The flow of ions that causes an IPSP or EPSP is an excitatory or inhibitory postsynaptic current (EPSC or IPSC).

A finely tuned balance in the activity of these cells is necessary for proper function of the brain. The developing nervous system of mammals is largely inaccessible and therefore, the processes guiding the establishment of this balance are difficult to investigate. Embryonic stem cells can be directed towards neuronal differentiation and form mature, synaptically connected neural networks in vitro. These networks also contain excitatory and inhibitory neurons and their interaction controls their patterns of activity.

The fact that stems cells can be induced to differentiate into neurons in-vitro and that these neurons form functioning networks opens the possibility to study the transition of precursor cells to mature neurons under controlled conditions in vitro.

Over the past 20 years, stem cell technologies have become an increasingly attractive option to investigate and treat neurodegenerative diseases that are characterized by the loss of neurons in the brain such as Parkinson’s disease.

Stem cells have unique properties that distinguish them from other type of cells. They have the capability of dividing and self-renewal for many generations through mitotic cell division while maintaining the undifferentiated state. They usually arising from a single cell and have the ability to differentiate into all possible specialised cell types. Embryonic stem cells (ES) are pluripotent, derived from the inner cell mass of an early stage embryo the blastocyst, 5-6 days post fertilization. They are able to differentiate into tissue of the three primary germ layers: ectoderm, endoderm and mesoderm but they can also be maintained in an undifferentiated state for a prolonged period in culture. ES cells can be identified by transcription factors such as Nanog and Oct4. There are different classifications of stem cells that reflect the range of possible cell types they can produce, and the ways in which the stem cells are derived. These include embryonic stem (ES) cells, progenitor cells, mesenchymal stem cells (MSCs), and induced pluripotent stem (iPS) cells.

More recently, the development of iPS cells provide an additional source of autologous stem cells for modeling and treating diseases. iPS cells are generated from somatic tissue such as fibroblasts and are reprogrammed into ES-like cells by the addition of select transcription factors: Oct 3/4, Klf, Sox2 and c-Myc. (Okita and Yamanaka 2011)

We used for our experiments mES cell derived-neurons which from synaptically connected networks in vitro. The functional connectivity of such networks can be analysed by using electrophysiological methods. The results of such studies have implications for basic and clinical research especially the genetics of neuropsyciatric disorders has increased interest into neuronal development. A big advantage of in vitro studies is the production of an unlimited number of cells. This raise the possibility to carry out parallel investigations and comparison of different genetic backgrounds and when necessary under pharmacological conditions.

We were interested to study developmental stages in different cell lines and compare their functional characteristics from a progenitor cell to an immature neuron which finally becomes a mature neuron. We compared neuronal properties as resting membrane potential (RMP), occurrence of voltage-gated channels, ability to fire action potentials (AP) up to functioning neuronal networks due to synaptic activity (sEPSCs and sIPSCs).

II. Chapter 1

Functional characterization of stem cell derived-neurons from different backgrounds

Lydia Barth[1], Rosmarie Sütterlin[1], Markus Nenniger[1] and Kaspar Vogt[1*]

1
Neurobiology/Pharmacology
Biozentrum
University of Basel
Klingelbergstrasse 50/70
4056 Basel
Switzerland

1. Abstract

Murine stem cell derived-neurons have been used to study a wide variety of neuropsychiatric diseases with a hereditary component, ranging from autism to Alzheimer's. While a significant amount of data on their molecular biology has been generated, there is little data on the physiology of these cultures. Different mouse strains show clear differences in behavioural and other neurobiologically relevant readouts. We have studied the physiology of early differentiation and network formation in neuronal cultures derived from three different mouse embryonic stem cell lines. We have found largely overlapping patterns with some significant differences in the timing of the functional milestones. Neurons from R1 showed the fastest development of intrinsic excitability, while E14Tg2a and J1 were slower. This was also reflected in an earlier appearance of synaptic activity in R1 cultures, while E14Tg2a and J1 were delayed by up to two days. In conclusion, stem cells from all backgrounds could be successfully differentiated into functioning neural networks. Given the differences between cells from different lines, control cell lines should be carefully chosen when investigating genetic alterations that lead to subtle deficits in neuronal function.

2. Introduction

For a variety of neuropsychiatric disorders, disturbed development represents one of the most compelling hypotheses for their aetiology. In several cases, relatively mild defects in neuronal and synaptic signalling were found to be likely to cause the disease. For the vertebrate central nervous system (CNS) early developmental stages are difficult to investigate functionally, since the tissue is difficult to assess.

Murine embryonic stem (mES) cell derived neurons provide substantial methodological benefits for the study of such neuropsychiatric disorders, particularly with a hereditary component. Essentially unlimited numbers of identical cultures can be produced and the cultures provide ready access to a developing neural system. These cultures have provided useful insights into the early stages of neuronal differentiation (Bibel, Richter et al. 2007) and have allowed studying a wide range of diseases from Rett Syndrome to Parkinson's disease. Most of the investigators have used morphological, molecular and histochemical markers to describe their cultures. For several, especially neurodevelopmental disorders, such as autism, subtle networking deficits have been described (Ebert and Greenberg 2013) and are hypothesized to cause the disease. Physiological data on the development of mES cell derived neurons and neuronal networks are relatively scarce. We have therefore decided to investigate the physiology of developing neural networks formed by neurons derived from mES cells. Because different strains of mice have shown different neuropsychiatric phenotypes (Barkus 2013) (Scharf and Schmidt 2012) we have decided to investigate three different lines of mice: R1, E14Tg2a and J1. Together with their morphological development we investigated intrinsic neuronal parameters such as the resting membrane potential (RMP), the occurrence of voltage gated ion channels and the firing of action potentials (APs). We also studied the development of both excitatory and inhibitory synaptic contacts and their functional maturation.

3. Materials and methods

Cell culture and differentiation

Embryonic stem cells derived from three different wild type (wt) backgrounds R1, E14Tg2a and J1 were cultured and differentiated into neurons as described(Bibel, Richter et al. 2007). Briefly, after 4 days of embryoid body formation they are treated with 5 µM all-*trans*-retinoic acid (Sigma) for additional 4 days. Embryoid bodies are dissociated and neuronal precursors were plated on poly-L-ornithine (Sigma) /laminin (Roche) - coated glass cover slips (Assistent). At day in vitro (DIV) 0 and 1 neuronal precursors were cultured in neural medium containing DMEM/F12, N-2 Supplement (100X) and penicillin/streptomycin and 1 mM glutamine (all Invitrogen). From DIV 2 the medium was changed to the differentiation medium containing Neurobasal medium, B-27 ® Supplement (50X), N-2 Supplement (100X), 0.6 mM glutamine and penicillin/streptomycin (all Invitrogen).

Electrophysiology

Cover slips with neurons were transferred to a bath chamber mounted to an inverse microscope (Axiovert 25, Carl Zeiss, Germany). Experiments were performed on DIV 0-8 and DIV 11-23 neurons in culture using a whole-cell voltage-clamp technique. Data were obtained using a Multiclamp 700A amplifier (Axon Instruments, USA). We used electrodes with an open tip resistance of 4-5 MΩ obtained by pulling borosilicate pipettes with 1.5 mm external diameter and 1.17 mm internal diameter without filament to a tip diameter of $\sim$1 μm on a horizontal Puller (DMZ Puller, Zeitz GmbH, Germany). The intracellular solution was adapted to the culture medium the cells were cultivated in; for N2 medium it contained (mM): 110 K-D-gluconate, 5 KCl, 11 Tris-phosphocreatine, 1 EGTA, 4.5 MgATP, 10 HEPES, 0.3 Tris-GTP (pH 7.4 with KOH, 290 mOsm). The extracellular solution for cells coming from N2 medium used for DIV 0 and DIV 1 contained (in mM): 120 NaCl, 29 $NaHCO_3$, 4 KCl, 1 $CaCl_2$, 0.7 $MgCl_2$, 18 glucose, pH 7.4 when bubbled continuously with 95% O_2 and 5% CO_2. Intracellular solution for cultures coming from complete medium contained (mM): 100 K-D-gluconate, 5 NaCl, 1 EGTA, 5 MgATP, 10 HEPES, and 0.5 Tris-GTP (pH 7.4 with KOH, 210 mOsm). The extracellular solution for complete medium contained (in

mM): 125 NaCl, 26 $NaHCO_3$, 1.25 $NaH_2PO_4*H_2O$, 2.5 KCl, 1.0 $MgSO_4$, 2.0 $CaCl_2$ and 11 glucose, pH 7.4 when bubbled continuously with 95% O_2 and 5% CO_2. Voltage-gated sodium- and potassium channels were detected in voltage- clamp mode at a holding potential of -60 mV. The holding potential was changed in a stepwise fashion from -75 mV to +25 mV in 5 mV increments and the voltage-gated peak inward current and maximal sustained outward current were measured. The inward currents were tetrodotoxin (TTX) sensitive, while the outward currents were blocked by tetraethyl-ammonium (TEA) (3 mM) and 4-aminopyridine (4-AP) (1 mM). Resting membrane potentials (RMP) and action potentials (APs) were recorded in current-clamp mode. Somatic current injections were applied in 2.5 pA steps from -2.5 pA to +30 pA. Synaptic activity was measured in voltage-clamp mode: to detect spontaneous excitatory synaptic currents (sEPSCs), cells were held at –60 mV, while for spontaneous inhibitory synaptic currents (sIPSCs), cells were held at -40 mV. Responses were filtered at 5 kHz and digitized at 20 kHz. The excitatory glutamate receptor blocker 2,3-dihydroxy-6-nitro-7-sulfamoyl-benzo[f]quinoxaline-2,3-dione (NBQX) (10 µM) and antagonists of inhibitory $GABA_A$ receptors picrotoxin (100 µM) or bicuculline (20 µM) were added to the perfusate to block the respective synaptic activity. Recorded sEPSC and sIPSC were detected and analysed using Mini Analysis 6 (Synaptosoft, USA). All other data analysis was done with IGOR PRO 6.0 (Wavemetrics, USA) software. Two-way ANOVA were used for all statistical analysis (unless otherwise mentioned), with post hoc Bonferroni tests where indicated.

Immunocytochemistry

Cells cultured on glass coverslips were rinsed twice with PBS pH 7.4 and fixed with 10% neutral buffered formalin (Sigma) for 20 min at RT. After rinsing with PBS, coverslips were permeabilized for 5 min in 0.2% TritonX-100/PBS, rinsed with PBS and incubated for 1 h at RT in a humidified chamber with the following primary antibodies and dilutions (rb: rabbit, ms mouse) : doublecortin (rb, 1:1000, Cell Signaling), microtubule-associated protein 2 (MAP2) (rb, 1:1000, Chemicon) and synaptophysin (ms, 1:300, Sigma). After several washes with PBS, coverslips were incubated for 1 h at RT with corresponding secondary antibody: Cy3 (goat anti rabbit

IgG (H+L) 1:1000**,** Cy5 (goat anti rabbit IgG (H+L), 1:200, (Immuno Jackson), Alexa 488-phalloidin, 1:400, (Molecular Probes) and DAPI (1:1000, Molecular Probes). After several washes in PBS, coverslips were mounted in Mowiol-1188 as previously described (Baschong, Duerrenberger et al. 1999). Confocal sections were recorded with a confocal laser scanning microscope Leica TCS SPE with DMI 4000B and processed with Imaris software and Adobe Photoshop version 10.0.

4. Results

We differentiated R1, E14Tg2a and J1 stem cells all from different wt backgrounds into neurons using an established protocol for mES cells (Bibel, Richter et al. 2007). Progenitor cells showed already on DIV 0 a distinct, spindle shape morphology (Figure 1A). Over the course of further development all cells acquired a distinct multipolar shape (Figure B-D). We followed the morphological development from DIV 0 to DIV 6 using R1 cells as an example. Cells were immunostained with antibodies against the nuclear marker DAPI (Figure 1 E-H), the neuronal marker doublecortin (Figure 1 I-L) and stained with the actin cytoskeleton label phalloidin (Figure 1 M-O). These stainings reveal that on DIV 1 85% of cells expressed doublecortin and this fraction rose to >90% by DIV 6. This developmental pattern was found in all stained cultures.

We next investigated key physiological parameters of neuronal maturation. We obtained patch-clamp recordings from cells throughout their neuronal differentiation from DIV 0 to DIV 13. Cells were held in the current-clamp configuration and their RMP was recorded; somatic current injection was then used to investigate AP firing in the developing neurons (Figure 2 A-D).

Cells usually started firing immature single APs at DIV 3; by DIV 6 most neurons produced repetitive mature action potentials upon a 0.8 s depolarizing pulse. The same cells were subsequently held in the voltage-clamp configuration and the functional expression of voltage-gated conductances was studied (Figure 2 E-H). Depolarizing current pulses produced two types of currents: fast activating and inactivating inward currents and slow activating outward currents with little inactivation. Inward currents were blocked by the sodium channel blocker TTX (1 µM), while outward currents were sensitive to the potassium channel blockers TEA (3 mM) and 4-AP (1 mM).

In cells from all backgrounds RMP development followed a characteristic time-course. After an initial hyperpolarized phase at DIV 0 cells depolarized over the following days and started hyperpolarizing again from DIV 5 (Figure 3 A). By DIV13 neurons in culture showed a mature, hyperpolarized RMP of -64 mV ± 1.8 mV for R1, -58 mV ± 2.7 mV for E14Tg2a and -57 mV ± 2.0 mV for J1 cultures. Statistical analysis revealed a highly significant influence ($p<0.01$) of developmental age and of

the cell type on RMP, but no interaction between the two variables (N>15) measurements per day and background; two-way ANOVA). Post-hoc comparisons (Bonferroni test) show that changes in RMP are largest for early time-points. Significant differences between genotypes were restricted to DIV 0. Voltage-dependent sodium currents show a monotonous increase in amplitude from DIV 0 to DIV 13 in cells from all backgrounds (Figure 3 B). We found a highly significant ($p<0.01$) influence of DIV and background on the amplitude of voltage-gated sodium currents - the interaction between the two variables was also highly significant ($p<0.01$) (N=25 per cell type and day; two-way ANOVA). The difference between backgrounds was significant for DIV 0 (post-hoc Bonferroni test).

In cells from all backgrounds, voltage-dependent potassium currents showed an early increase that levelled at around 1.5 nA at DIV 8 (Figure 3 C). Again the current amplitude was highly significantly dependent on DIV and background with a significant interaction between the two ($p<0.01$ for all, N=25 per cell type and day, two-way ANOVA). In post-hoc comparisons the influence of the background was restricted to DIV 0 ($p<0.05$, Bonferroni test).

To study AP generation by the developing neurons, we depolarized cells above threshold by somatic current injection in current-clamp mode. In very young cells, either no active depolarization or only an immature spike was detected (see Figure 2 B&C). As the cultures matured the APs grew significantly in size (Figure 4 A) ($p<0.01$) and became significantly faster (Figure 4 B) ($p<0.01$, N=103 for both parameters, Two way ANOVA). By DIV 6, most cells fired repetitive fast APs (see Figure 2 D) during a 0.8 s long depolarizing pulse. There was no significant dependence of the peak AP frequency (Figure 4 C) ($p>0.40$, N=95, two-way ANOVA) or of the amount of frequency adaptation (Figure 4 D) on DIV ($p>0.93$, N=89, two-way ANOVA). When comparing cells from different backgrounds we found a highly significant influence of the cell type on AP half-width and on the peak AP frequency ($p<0.01$; N=94 for each cell type, two-way ANOVA).

We looked for spontaneous synaptic events in voltage-clamp recordings from cell beginning with DIV 8. At DIV 8 none of the recorded cells showed any synaptic activity (N=10 for the different backgrounds). We detected the first spontaneous excitatory (sEPSCs) and inhibitory (sIPSCs) postsynaptic currents by DIV 9 in R1

(N=15) neurons, by DIV10 in J1 (N=6) and by DIV11 in E14Tg2a (N=15) neuronal cultures (Figure 5). We measured sEPSCs as inward currents (Figure 5 E-H, bottom traces) at a holding potential of -60 mV, while sIPSCs were best visible and measured as outward currents at a holding potential of -40 mV (Figure 5 E-H, top traces). Inward currents were blocked by the addition of the AMPA-receptor blocker NBQX (10 µM) to the perfusate (Figure 5 J), whereas the outward currents were blocked by bath application of the $GABA_A$ receptor antagonist picrotoxin (100 µM) (Figure 5 K) in all cultures tested. Spontaneous synaptic activity was sensitive to the application of the sodium channel blocker TTX (1 µM) (Figure 5 L&M).

Apart from the different ages of onset there was no significant difference in the number of either sEPSCs or sIPSCs between cells from different backgrounds (Figure 5 N&O) (N=178, two-way ANOVA). Punctate labeling for the synaptic marker synaptophysin could be observed in close contact to the postsynaptic label MAP2 (Figure 5 A-D) in R1 mES cell derived cultures. Such stainings were observed in all cultures tested (data not shown).

5. Discussion

Here we show that mES cells derived-neurons mature within less than two weeks in culture and form functional, synaptically connected networks around DIV 11. Neurons undergo a relatively stereotypical development; thus, for the lines tested here the exact background of the mES cells is not a decisive factor when designing such experiments. For all of the parameters measured, we observed a considerable variability from cell to cell and from culture to culture, necessitating a large number of measurements to determine a given data point. The RMP shows an interesting biphasic behavior: From an initially hyperpolarized state cells undergo transient depolarization and then gradually repolarize to values that are typical for mature neurons. While the overall behavior is the same for cells derived from different mES backgrounds, there are significant differences in the time-course for the different lines. Rudimentary APs were detected surprisingly early during development, however mature overshooting spikes were reliably evoked only in cultures from DIV 6. The maturation in AP-shape was paralleled by the increasing function of voltage-gated conductances in these cultures. Both voltage-gated sodium-, as well as potassium conductances showed a several fold increase in amplitude over the time studied. Again, cells from different backgrounds showed the same general pattern with significant differences in timing early on. Excitatory and inhibitory synaptic events were detected at the same time for cultures from the same background. Arguing against an accelerated maturation of one type of connectivity, as has been described for several in-vivo situations (Ben-Ari 2002). Spontaneous APs contribute to synaptic activity, as the effect of TTX on spontaneous synaptic events shows. The occurrence of synaptic activity did not parallel the different speed at which voltage-gated conductances developed. Cultures from J1 background were delayed in their development of voltage-gated conductances, but showed synaptic activity early on, while cells from E14Tg2a background developed their voltage gated conductances relatively fast, but were delayed in showing synaptic activity compared to cells from other backgrounds. This indicates that the differences between cultures from different backgrounds are not due to a ‘master-clock’ running at different speeds, but rather a subtly different developmental pattern in the different mES strains. While the differences in developmental timing were relatively small, they can become significant and this may affect the comparison between wild-type and

mutated neurons, if the control neurons are not derived from the same background. Compared to differentiating murine neurons in situ, measured in timed acute brain slice preparations, the mES derived-neurons showed similar developmental milestones. For voltage-gated sodium- (I_{Na} 1.7 nA in mES versus 0.8 nA in situ) and potassium currents (I_K 1.3 nA in mES and 1.2 nA in situ) (Picken Bahrey and Moody 2003)similar mature values were reached and the resulting APs were also very similar in the development of their kinetics. In situ neurons took 19 days (E14 to P12) to mature, while mES cell derived-neurons took 16 days (4 days of retinoic acid treatment followed by plating and 12 days of maturation) to reach comparable developmental stages (Picken Bahrey and Moody 2003). This indicates that the development of the intrinsic neuronal physiology is surprisingly faithfully reproduced by mES cell derived neurons. In comparison to neurons derived from neural stem cells (NS) expanded after differentiation from mES (Biella, Di Febo et al. 2007) our cells, which do not undergo further expansion, develop more rapidly. They produce repetitive fast action potentials at DIV 6, while the NS derived neurons reach that milestone not before DIV 10 or possibly later.

Neurons differentiated from mES cells show a robust developmental pattern across several strains of ES cells and form mature neural networks within a time frame comparable to the in-vivo situation. This makes mES cell derived-neuronal cultures an easily accessible system that can be easily treated with different pharmacological compounds or modulators of gene expression. The small, but significant differences in the developmental time course indicate that for experiments with genetically modified cell lines, control and mutated cells should come from the same background when comparing subtle differences in neuronal maturation.

6. References

Barkus, C. (2013). "Genetic mouse models of depression." Current topics in behavioral neurosciences **14**: 55-78.

Baschong, W., M. Duerrenberger, et al. (1999). "Three-dimensional visualization of cytoskeleton by confocal laser scanning microscopy." Methods in enzymology **307**: 173-189.

Ben-Ari, Y. (2002). "Excitatory actions of gaba during development: the nature of the nurture." Nature reviews. Neuroscience **3**(9): 728-739.

Bibel, M., J. Richter, et al. (2007). "Generation of a defined and uniform population of CNS progenitors and neurons from mouse embryonic stem cells." Nature protocols **2**(5): 1034-1043.

Biella, G., F. Di Febo, et al. (2007). "Differentiating embryonic stem-derived neural stem cells show a maturation-dependent pattern of voltage-gated sodium current expression and graded action potentials." Neuroscience **149**(1): 38-52.

Ebert, D. H. and M. E. Greenberg (2013). "Activity-dependent neuronal signalling and autism spectrum disorder." Nature **493**(7432): 327-337.

Picken Bahrey, H. L. and W. J. Moody (2003). "Early development of voltage-gated ion currents and firing properties in neurons of the mouse cerebral cortex." Journal of neurophysiology **89**(4): 1761-1773.

Scharf, S. H. and M. V. Schmidt (2012). "Animal models of stress vulnerability and resilience in translational research." Current psychiatry reports **14**(2): 159-165.

7. Figure Legend

Figure 1: Derivation of neurons from mouse embryonic stem cells

A-D) DIC images of early neuronal differentiation of R1 stem cell derived cultures. A) Progenitor cells 6h after plating; B) at DIV 1; C) at DIV 3 and D) at DIV 6. E-O) Immunostainings against neuronal markers at the corresponding DIV. E-H) nuclear staining with DAPI; I-L) labeling against the marker for immature neurons doublecortin; M-O) actin staining with phalloidin; Scale bar: 20 µm.

Figure 2: Characterization of intrinsic parameters in immature developing neurons

Early development of neuronal physiology; the numbers next to the traces indicate the resting membrane potential. A-D) Reaction of R1 neurons to negative (bottom traces) and positive (top traces) somatic current injections at A) DIV 0; B) DIV 1; C) DIV 3 and D) DIV 6. E-H) Sample traces and I-V curves for voltage-activated inward sodium currents (red) and voltage-activated outward potassium currents (black). Data points for the I-V curves plot peak inward current (red squares) against the holding potential after depolarization and the sustained outward current (black dots) against the holding potential after depolarization. Corresponding time points: E) DIV 0; F) DIV 1; G) DIV 3 and H) DIV 6 top insert currents under baseline condition and bottom insert currents after bath application of TTX (1 µM) and 4AP (1 mM).

Figure 3: Developmental characterization of resting membrane potential and voltage gated sodium- and potassium currents

A) Comparison of resting membrane potential (RMP) from DIV 0-13 of neurons derived from R1 (black), E14T2ga (grey) and J1 (light grey) mES cells. B) Comparison of inward sodium currents as a function of developmental age from DIV 0-13 in neurons derived from R1 (black), E14T2ga (grey) and J1 (light grey) mES cells. C) Comparison of outward potassium currents as a function of developmental age from DIV 0-13 in neurons derived from R1 (black), E14T2ga (grey) and J1 (light grey) mES cells.

Figure 4: Neuronal spiking patterns as a function of developmental age

A-D) Analysis of the spiking parameters in neurons derived from of R1 (black), E14T2ga (grey) and J1 (light grey) mES cells as a function of time from DIV 0-13 in culture. A) Data for the amplitude of the first AP, B) the half-width at half height for the first AP, C) the initial firing frequency and D) the frequency at the end of the train relative to the initial firing frequency.

Figure 5: Development of synaptic activity

Morphology of synaptic contacts: DIC A) and immunostainings B-D) of DIV 12 R1 cells against the presynaptic marker synaptophysin B), the neuronal marker MAP2 C) and overlay of both D). Scale bar: 20 µm. E-H) Traces of spontaneous synaptic activity of R1 cells in voltage-clamp from DIV 8, DIV 9, DIV 10 and DIV 12. Top traces at -40 mV holding potential, bottom traces at -60 mV respectively. I-K) Pharmacological characterization of synaptic currents. I) Sample trace of one experiment with baseline recording J) after bath application of NBQX (10 µM) and K) bath application of picrotoxin (100 µM). L) Sample trace of spontaneous synaptic activity under control conditions and M) after the application of TTX (1 µM). N) Frequency of sEPSCs as a function of DIV for neurons derived from R1 (black), T2ga (grey) and J1 (light grey) mES cells in cultures from DIV 8-13 O) Same data for sIPSCs.

8. Figures

Figure 1

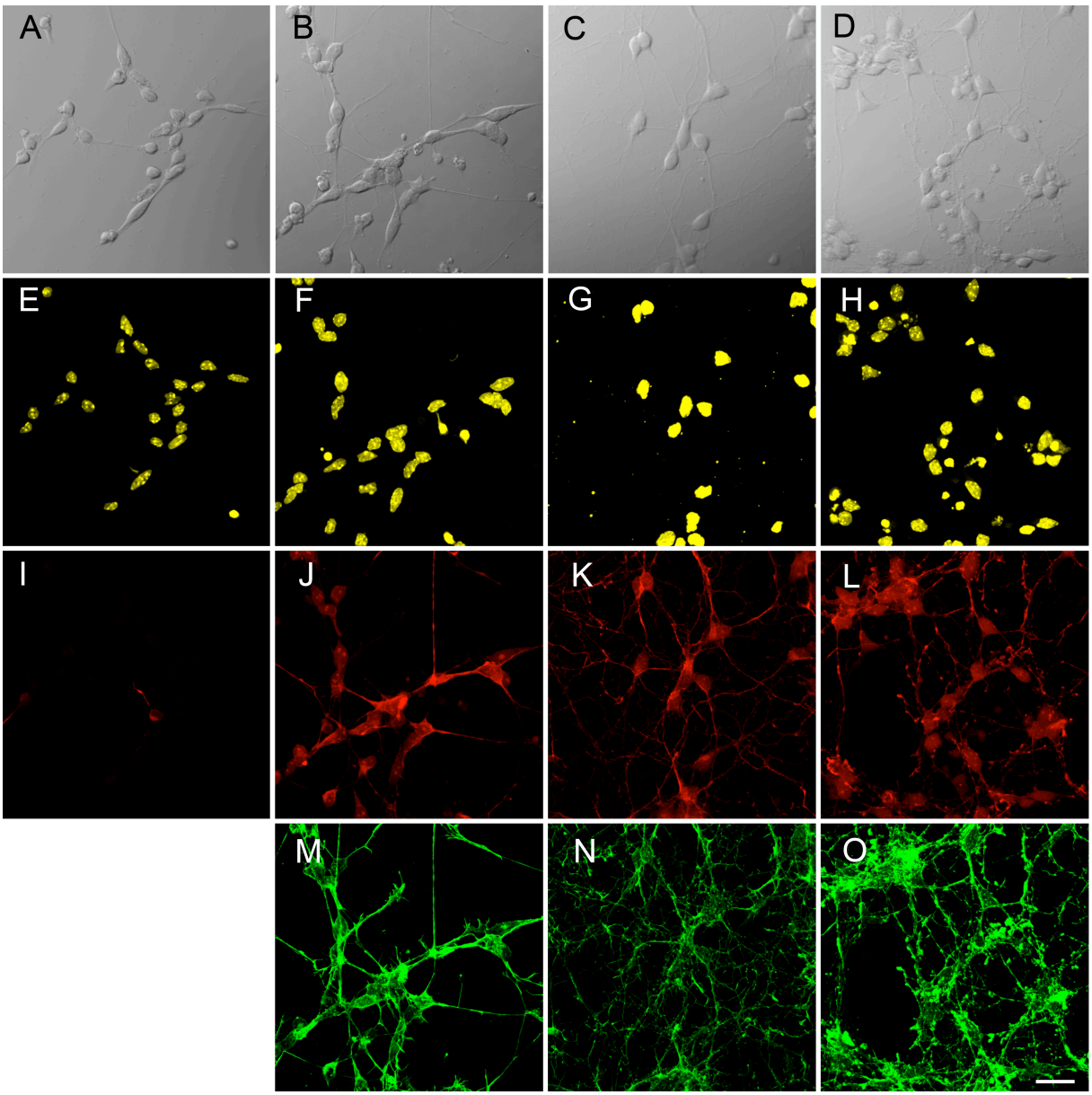

Figure 2

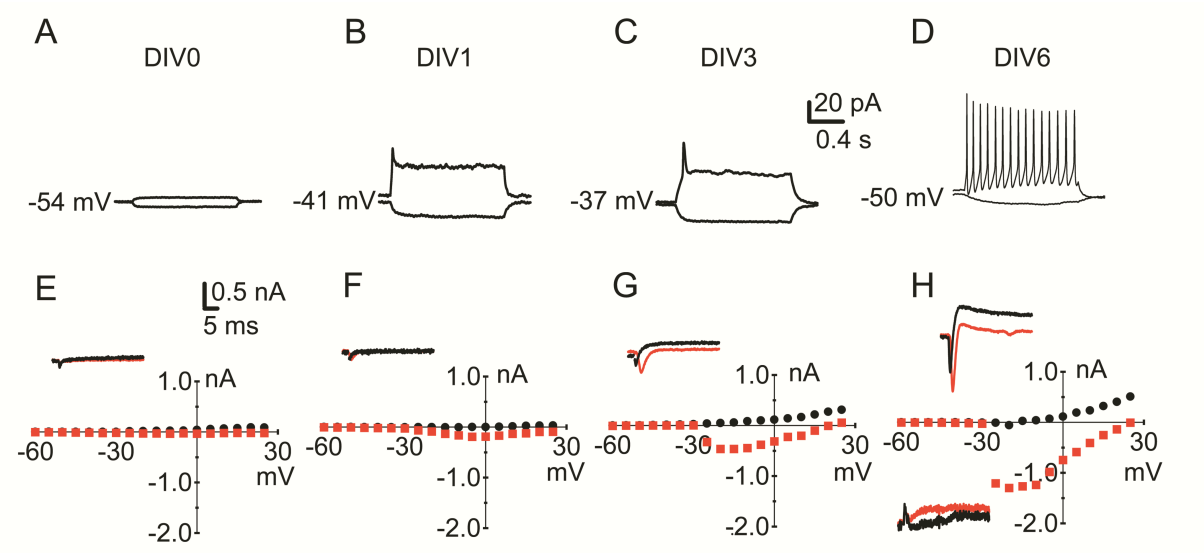
A
DIV0
-54 mV
B
DIV1
-41 mV
C
DIV3
-37 mV
20 pA
0.4 s
D
DIV6
-50 mV
E
0.5 nA
5 ms
1.0 nA
-60
-30
30
mV
-1.0
-2.0
F
G
H

Figure 3

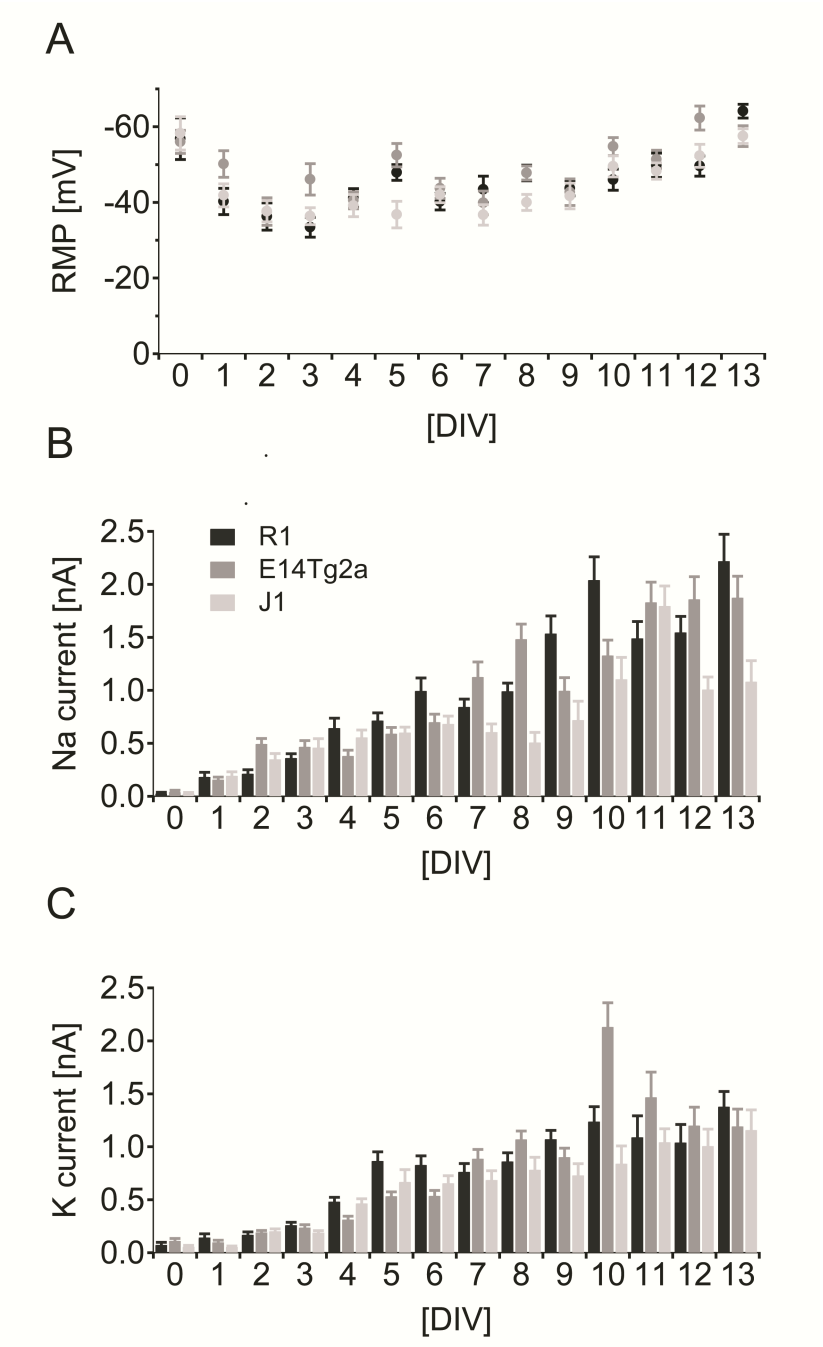
A
RMP [mV]
-60
-40
-20
0
0 1 2 3 4 5 6 7 8 9 10 11 12 13
[DIV]
B
Na current [nA]
2.5
2.0
1.5
1.0
0.5
0.0
R1
E14Tg2a
J1
0 1 2 3 4 5 6 7 8 9 10 11 12 13
[DIV]
C
K current [nA]
2.5
2.0
1.5
1.0
0.5
0.0
0 1 2 3 4 5 6 7 8 9 10 11 12 13
[DIV]

Figure 4

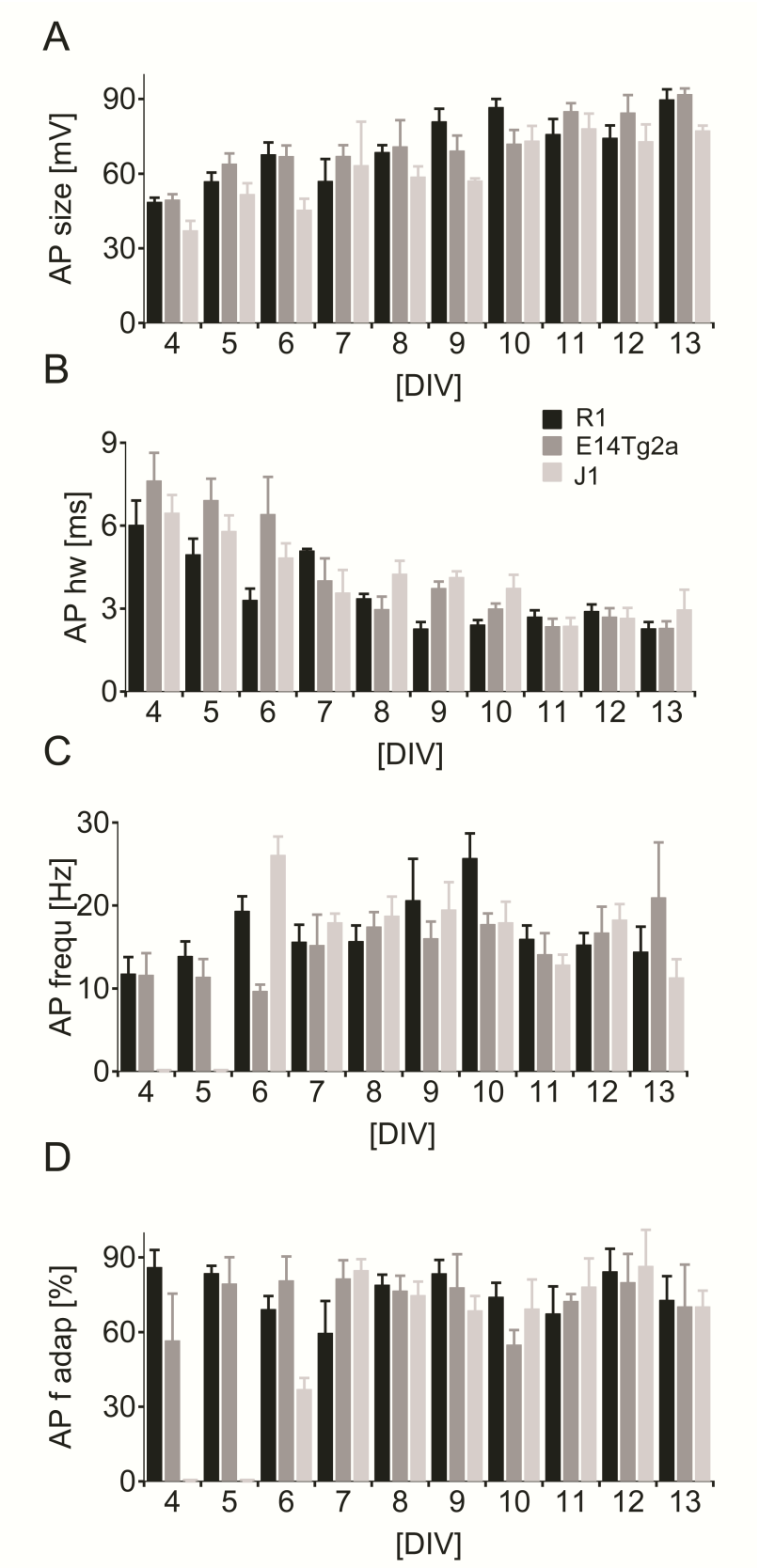
A
AP size [mV]
0
30
60
90
4 5 6 7 8 9 10 11 12 13
[DIV]
B
AP hw [ms]
0
3
6
9
R1
E14Tg2a
J1
4 5 6 7 8 9 10 11 12 13
[DIV]
C
AP frequ [Hz]
0
10
20
30
4 5 6 7 8 9 10 11 12 13
[DIV]
D
AP f adap [%]
0
30
60
90
4 5 6 7 8 9 10 11 12 13
[DIV]

Figure 5

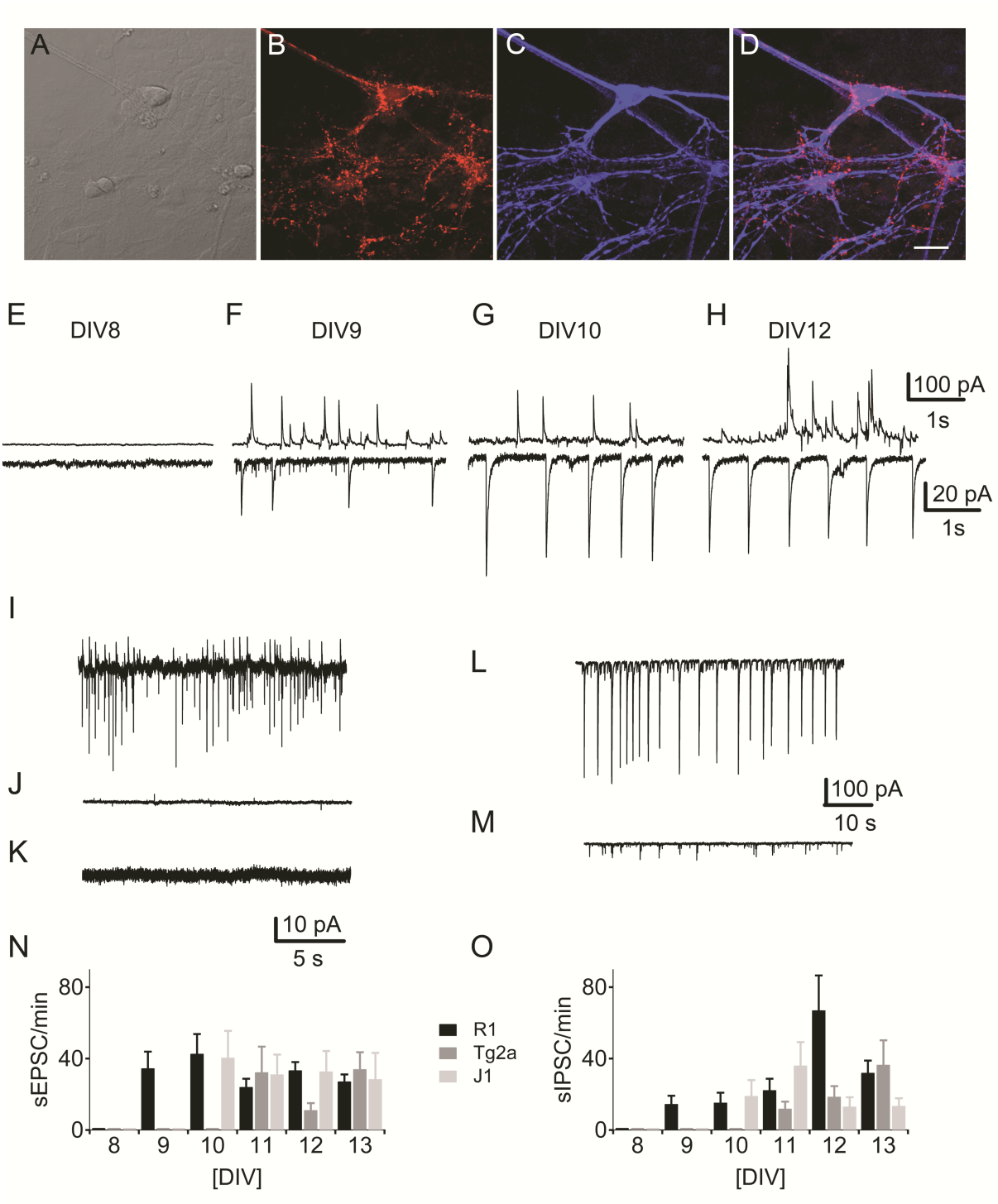
A
B
C
D
E
DIV8
F
DIV9
G
DIV10
H
DIV12
100 pA
1s
20 pA
1s
I
J
K
L
100 pA
10 s
M
N
10 pA
5 s
sEPSC/min
80
40
0
8
9
10
11
12
13
[DIV]
R1
Tg2a
J1
O
sIPSC/min
80
40
0
8
9
10
11
12
13
[DIV]

III. Chapter 2

Reduced synaptic activity in MeCP2 deficient neuronal networks derived from embryonic stem cells

Running title: MeCP2 and synaptic activity

Lydia Barth[1], Rosmarie Sütterlin[1], Markus Nenniger[1] and Kaspar Vogt[1*]

1
Neurobiology/Pharmacology
Biozentrum
University of Basel
Klingelbergstrasse 50/70
4056 Basel
Switzerland

1. Abstract

Neurodevelopmental diseases such as the Rett syndrome have received renewed attention, since the mechanisms involved may underlie a broad range of neuropsychiatric disorders such as schizophrenia and autism. In vertebrates early stages in the functional development of neurons and neuronal networks are difficult to study. Embryonic stem cell-derived neurons provide an easily accessible tool to investigate neuronal differentiation and early network formation. We used in vitro cultures of neurons derived from murine embryonic stem cells missing the MECP2 gene (MeCP2-/y) and from E14Tg2a wild type cells. We studied the functional maturation of the developing neurons and the activity of the synaptic connections they formed. Neurons exhibited minor differences in the developmental patterns for their intrinsic parameters, such as resting membrane potential and excitability; with the MeCP2-/y cells showing a slightly accelerated development. When measuring synaptic activity we found no difference in the early phase of development, but as the cultures matured, significant deficits became apparent, particularly for inhibitory synaptic events. Embryonic stem cell-derived neuronal cultures show clear developmental deficits that match phenotypes observed in slice preparations and thus provide a compelling tool to further investigate the mechanisms behind Rett syndrome pathophysiology.

Keywords: Rett syndrome; stem cell-derived neurons; neurodevelopment; electrophysiology; excitability; synaptic activity

2. Introduction

In 1966 the neurologist Dr. Andreas Rett described an unusual neurodevelopmental disorder in girls, now called Rett Syndrome (RTT) (Rett 1966). Today the key diagnostic criteria for RTT are stereotypic hand movements, deficits in motor coordination, speech disorders and autistic behavior (Hagberg and Hagberg 1997). Children develop normally for 6 to 18 months after birth, reaching the usual motor, language and social milestones. This brief period of developmental progress is followed by stagnation with growth arrest and microcephaly. During the following rapid regression phase, the previously acquired skills are lost and a variety of neurological symptoms develop including sleep disturbances, problems with gait, decelerated head growth, breathing arrhythmia, stereotypical hand movements, loss of motor coordination, and seizures, among them (Zoghbi 2003) (Moretti and Zoghbi 2006) (Chahrour and Zoghbi 2007).

In 1999 Amir *et al* (Amir, Van den Veyver et al. 1999) identified the primary cause of RTT as a defect in the *MECP2* gene on the X chromosome, coding for the methyl-CpG-protein2 (MeCP2). More than 95% of individuals with classic RTT carry a *de novo* mutation in the gene encoding MeCP2.

MeCP2 is highly enriched in neurons in the central nervous system (Zhou, Hong et al. 2006). It regulates genes essential for neuronal survival, dendritic growth, synaptogenesis, and synaptic plasticity (Fukuda, Itoh et al. 2005) (Smrt, Eaves-Egenes et al. 2007) (Chang, Khare et al. 2006). The function of MeCP2-targeted genes seems especially important in GABAergic neurons (Huang, Di Cristo et al. 2007). GABAergic interneurons provide the main inhibitory function in the central nervous system and thereby contribute to the essential balance between excitation and inhibition. A disturbed excitation/inhibition balance will in severe cases result in epileptic discharges, which are found in 70-90% of RTT patients (Nissenkorn, Gak et al. 2010).

Generation of different mouse models in 2001 by targeting of the *MECP2* gene has provided significant advances in understanding of MeCP2 function and mimicking relevant aspects of human RTT (Guy, Hendrich et al. 2001) (Chen, Akbarian et al. 2001) (Shahbazian, Young et al. 2002). MeCP2- null male mice (MeCP2-/y) were generated by replacing exons 3 and 4 of *MECP2* starting in early embryonic development (Guy, Hendrich et al. 2001). Most studies use such male hemizygous

mice because they develop a severe and characteristic behavioral phenotype much earlier than female heterozygous mice. The mice develop motor impairments, tremor, breathing abnormalities, limb stereotypies and epilepsy as in the human condition (Colic, Wither et al. 2013). Remarkably, it was later shown that re-expression of endogenous MeCP2 can reverse aspects of RTT in the adult (Guy, Gan et al. 2007). Within a few weeks the affected mice were largely indistinguishable from their wild type (wt) controls. This does not yet suggest a prompt therapeutic approach to RTT but it clearly establishes the principle of reversibility in this mouse model.

The causal link between MeCP2 dysfunction and the neurobehavioral phenotype is still unclear. Given the reversibility of the phenotype, a better understanding of the neuronal phenotype becomes more and more important. Especially early developmental stages are hard to study functionally since the neurons are difficult to reach at these stages.

Murine embryonic stem cell (mES)-derived neurons allow a straightforward functional analysis of neuron maturation from very early stages up to network formation.

Here we investigate the differentiation of neural precursors derived from MeCP2-/y mice and from the corresponding wild type. We compared intrinsic parameters, such as resting membrane potential (RMP), the function of voltage-gated sodium- and potassium channels as well as generation of action potentials (AP) from immature and mature neurons. As soon as the neurons formed synaptic networks, we studied spontaneous excitatory and inhibitory synaptic activity and its maturation over time.

3. Materials and methods

Cell culture and differentiation

Embryonic stem cells derived from a E14Tg2a background with the MeCP2+/y (wt) and MeCP2-/y genotype were cultured and differentiated into neurons as described (Bibel, Richter et al. 2007). Briefly, after 4 days of embryoid body formation they are treated with 5 µM all-*trans*-retinoic acid (Sigma) for additional 4 days. Embryoid bodies are dissociated and neuronal precursors were plated on poly-L-ornithine (Sigma) /laminin (Roche) - coated glass cover slips (Assistent). At DIV 0 and 1 neuronal precursors were cultured in neural medium containing DMEM/F12, N-2 Supplement (100X) and penicillin/streptomycin and 1 mM glutamine (all Invitrogen). From DIV 2 the medium was changed to the differentiation medium containing Neurobasal medium, B-27 ® Supplement (50X), N-2 Supplement (100X), 0.6 mM glutamine and penicillin/streptomycin (all Invitrogen).

Electrophysiology

Cover slips with neurons were transferred to a bath chamber mounted to an inverse microscope (Axiovert 25, Carl Zeiss, Germany). Experiments were performed on DIV 0-8 and DIV 11-23 neurons in culture using a whole-cell voltage-clamp technique. Data were obtained using a Multiclamp 700A amplifier (Axon Instruments, USA). We used electrodes with an open tip resistance of 4-5 MΩ obtained by pulling borosilicate pipettes with 1.5 mm external diameter and 1.17 mm internal diameter without filament to a tip diameter of $\sim$1 μm on a horizontal Puller (DMZ Puller, Zeitz GmbH, Germany). The intracellular solution was adapted to the culture medium the cells were cultivated in; for N2 medium it contained (mM): 110 K-D-gluconate, 5 KCl, 11 Tris-phosphocreatine, 1 EGTA, 4.5 MgATP, 10 HEPES, 0.3 Tris-GTP (pH 7.4 with KOH, 290 mOsm). The extracellular solution for cells coming from N2 medium used for DIV 0 and DIV 1 contained (in mM): 120 NaCl, 29 $NaHCO_3$, 4 KCl, 1 $CaCl_2$, 0.7 $MgCl_2$, 18 glucose, pH 7.4 when bubbled continuously with 95% O_2 and 5% CO_2. Intracellular solution for cultures coming from complete medium contained (mM): 100 K-D-gluconate, 5 NaCl, 1 EGTA, 5 MgATP, 10 HEPES, and 0.5 Tris-GTP (pH 7.4 with KOH, 210 mOsm). The extracellular solution for complete medium contained

(in mM): 125 NaCl, 26 $NaHCO_3$, 1.25 $NaH_2PO_4*H_2O$, 2.5 KCl, 1.0 $MgSO_4$, 2.0 $CaCl_2$ and 11 glucose, pH 7.4 when bubbled continuously with 95% O_2 and 5% CO_2. Voltage-gated sodium- and potassium channels were detected in voltage- clamp mode at a holding potential of -60 mV. The holding potential was changed in a stepwise fashion from -75 mV to +25 mV in 5 mV increments and the voltage-gated peak inward current and maximal sustained outward current were measured. The inward currents were tetrodotoxin (TTX) sensitive, while the outward currents were blocked by tetraethyl-ammonium and 4-aminopyridine (TEA (3 mM) and 4-AP (1 mM)) (data not shown). Resting membrane potentials and action potentials were recorded in current-clamp mode. Somatic current injections were applied in 2.5 pA steps from -2.5 pA to +30 pA, in older cells up to +60 pA. Synaptic activity was measured in voltage-clamp mode: to detect spontaneous excitatory synaptic currents (sEPSCs), cells were held at –60 mV, while for spontaneous inhibitory synaptic currents (sIPSCs), cells were held at -40 mV. Responses were filtered at 5 kHz and digitized at 20 kHz. The excitatory glutamate receptor blocker 2,3-dihydroxy-6-nitro-7-sulfamoyl-benzo[f]quinoxaline-2,3-dione (NBQX) (10 µM) and antagonists of inhibitory $GABA_A$ receptors picrotoxin (100 µM) or bicuculline (20 µM) were added to the perfusate to block the respective synaptic activity. Recorded sEPSC and sIPSC were detected and analysed using Mini Analysis 6 (Synaptosoft, USA). All other data analysis was done with IGOR PRO 6.0 (Wavemetrics, USA) software. Two-way ANOVA were used for all statistical analysis (unless otherwise mentioned), with post hoc Bonferroni tests where indicated.

Immunocytochemistry

Cells cultured on glass coverslips were rinsed twice with PBS pH 7.4 and fixed with 10% neutral buffered formalin (Sigma) for 20 min at room temperature (RT). After rinsing with PBS, coverslips were permeabilized for 5 min in 0.2% TritonX-100/PBS, rinsed with PBS and incubated for 1 h at RT in a humidified chamber with the following primary antibodies and dilutions (rb: rabbit, ms: mouse): doublecortin (rb, 1:1000, Cell Signaling), microtubule-associated protein 2 (MAP2) (rb, 1:1000, Chemicon), glutamic acid decarboxylase, 67 kDa isoform, (GAD67) (ms, 1:500, Chemicon) and synaptophysin (ms, 1:300, Sigma). After several washes with PBS,

coverslips were incubated for 1 h with corresponding secondary antibody: Cy5 (donkey anti rabbit IgG (H+L), 1:300, Immuno Jackson), Alexa 488 (donkey anti mouse IgG (H+L), 1:800, Invitrogen), Alexa 488-phalloidin (1:400, Molecular Probes) and DAPI (1:1000, Molecular Probes). After several washes in PBS, coverslips were mounted in Mowiol-1188 as previously described (Baschong, Duerrenberger et al. 1999). Confocal sections were recorded with a confocal laser scanning microscope Leica TCS SPE with DMI 4000B and processed with Imaris software and Adobe Photoshop version 10.0.

4. Results

Morphological development

We differentiated MeCP2+/y (wt) and MeCP2-/y mES cells from the same E14Tg2a background into neurons using an established protocol (Bibel, Richter et al. 2007). Progenitors dissociated from embryoid bodies (Figure 1a) showed already on DIV 0 a distinct, spindle shaped morphology (Figure 1b). To characterize their morphological development, wt (Figure 1 d-f) and MeCP2-/y cells (Figure 1 h-j) were stained on DIV 3 with antibodies against doublecortin (Figure 1 d, h), a marker of immature neurons. In addition we used the actin cytoskeleton label phalloidin (Figure 1 e, i) and the nuclear marker DAPI (Figure 1 f, j). By DIV 3 more than 90% of the cells in culture were immature neurons with a multipolar shape. The DAPI staining indicated that the cell densities were similar in both genotypes (wt: 21.4 ± 2.2 cells /10000 μm^2, N=10; MeCP2-/y: 21.8 ± 3.0 cells /10000 μm^2, N=10).

Functional development of voltage-gated currents

The wt progenitors exhibited a RMP of -56 mV ± 2.2 at DIV 0 (N=15) compared to -35 mV ± 3.0 for MeCP2-/y progenitors (N=8). At DIV 2 RMP of wt cells (N=21) decreased to -41 ± 3.3 mV, while for MeCP2-/y (N=16) we measured a RMP of -36 ± 2.1 mV. In the following days cells from both genotypes showed a gradual hyperpolarization to -57 ± 0.9 mV for wt and -57 ± 1.0 mV for MeCP2-/y, which stabilized around DIV 11 (N=180 for wt and 151 for MeCP2-/y). Statistical analysis revealed a highly significant influence of developmental age ($p<0.01$), but no significant effect of the genotype ($p>0.08$) on the RMP.

We observed voltage-dependent inward sodium currents (I_{Na}) with fast activation and inactivation kinetics, as well as slow, non-inactivating outward potassium currents (I_K) during all stages of differentiation. Already 6 h after plating in 6 of 10 cells a small I_{Na} of 0.04 ± 0.02 nA in wt and 0.02 ± 0.01 nA in MeCP2-/y and a I_K of 0.11 ± 0.03 nA in wt and 0.04 ± 0.01 nA in MeCP2-/y could be found. Both types of currents showed a substantial increase during development in culture (Figure 2). I_{Na} increased continuously from 0.48 ± 0.04 nA in wt and 0.60 ± 0.04 nA in MeCP2-/y (DIV 3-5) to 3.06 ± 0.16 nA in wt and 3.14 ± 0.23 nA in MeCP2-/y (DIV 20-23) (Figure 2e). For I_K

an initial increase from 0.36 ± 0.025 nA in wt and 0.45 ± 0.03 nA in MeCP2-/y (DIV 3-5) to 1.24 ± 0.07 nA in wt and 1.78 ± 0.11 nA in MeCP2-/y (DIV 11-14) then levelled off at 1.52 ± 0.09 nA in wt and 1.31 ± 0.09 nA in MeCP2-/y (DIV 20-23) (Figure 2f). For I_{Na} the effect of the genotype was not significant ($p>0.82$), while the developmental age exerted a highly significant effect ($p<0.01$) (N=25 per day and genotype). Both genotype and developmental age significantly affected I_K ($p<0.01$ for both variables, N=25 per day and genotype). Pairwise post-hoc analysis did not reveal a significant difference between genotypes at any specific time point ($p>0.5$).

Action potentials and excitability

Action potentials were detected from DIV 3 (Figure 1l) in both genotypes. Typical APs are shown for DIV 6 (Figure 3a), DIV 12 (Figure 3b) and DIV 21 (Figure 3c). A quantitative analysis of the APs was performed between the age ranges DIV 4-6, DIV 11-13 and DIV 20-23 in 61 wt and 44 MeCP2-/y cells (Figure 3 d-g) by measuring the size of the first AP in a train (see Figure 1m) and its half-width, as well as the initial frequency of APs in a train and their frequency adaptation. First AP size (Figure 3d) increased from DIV 4 to DIV 23 in wt neurons from 59.5 ± 2.5 mV to 87.6 ± 3.7 mV and in MeCP2-/y from 60.3 ± 4.9 mV to 95.7 ± 2.8 mV. First AP half width (Figure 3e) decreased over time in wt from 6.7 ± 0.5 ms to 2.2 ± 0.3 ms and in MeCP2-/y from 4.4 ± 0.7 ms to 1.6 ± 0.08 ms. Initial AP frequency within a train (Figure 3f) showed no clear developmental pattern and varied between 10-20 Hz for both genotypes. Cells from both genotypes exhibited a weak frequency adaptation to between 60% and 90% of the initial frequency (Figure 3g) throughout their development. Statistical analysis revealed a significant effect of age ($p<0.0.1$), but not of genotype ($p>0.3$) on AP size. Both age and genotype significantly affected the AP half-width ($p<0.01$) with a significant interaction ($p<0.01$). Initial AP frequency was significantly affected by both age ($p<0.01$) and genotype ($p<0.05$) without significant interaction ($p>0.2$). AP frequency adaptation was significantly affected by age ($p<0.05$), but not by genotype ($p>0.9$).

Synaptic activity

We detected the first spontaneous excitatory (sEPSCs) and inhibitory (sIPSCs) postsynaptic currents by DIV 11 in neurons from both wt and MeCP2-/y cultures (Figure 4). We measured sEPSCs as inward currents (Figure 4 a-c bottom traces) at a holding potential of -60 mV, while sIPSCs were best visible and measured as outward currents at a holding potential of -40 mV (Figure 4 a-c top traces). sEPSCs were blocked by the addition of the AMPA-receptor blocker NBQX (10 µM) to the bath medium, whereas sIPSCs were blocked by bath application of the $GABA_A$ receptor antagonists picrotoxin (100 µM) or bicuculline (20 µM) respectively, in all cultures tested (N=21) (Figure 4d).

Between DIV 11-23 the frequency of sEPSCs increased from 26.2 ± 4.8 to 71.8 ± 7.4 events per minute in wt (N=186) and from 21.2 ± 2.6 to 43.8 ± 4.6 events per minute in MeCP2-/y (N=172) (Figure 4e). This represents a highly significant increase with age ($p<0.01$) as well as a significant reduction in excitatory activity in MeCP2-/y cultures compared to wt ($p<0.05$).

The frequency of sIPSCs rose from 23.5 ± 5.1 to 97.8 ± 13.3 events per minute between DIV 11-23 for wt neurons, while in neurons from MeCP2-/y cultures it went from 19.7 ± 3.4 to 58.8 ± 7.9 events per minute over the same time (Figure 4f). Both developmental age ($p<0.01$) and the cell's genotypes ($p<0.01$) exerted a highly significant influence in inhibitory synaptic activity.

To see whether the reduced synaptic activity was accompanied by a change in synaptic density we stained cultures at DIV 12, 18 and 21 with antibodies against the neuronal marker MAP2 and against the presynaptic marker synaptophysin (Figure 5a-f). We measured synapse density by counting the number of synaptophysin positive puncta along 6-12 MAP2-positive dendrites per age range and genotype. In wt cultures the densities were 61 ± 2.2, 89 ± 8.9 and 64 ± 8.1 puncta/100 µm at DIV 12, 18 and 21 respectively. In MeCP2-/y cultures the values were 46 ± 2.6, 76 ± 7.3 and 81 ± 7.1 puncta/100 µm for the same time points (Figure 5m). While age had a significant influence on the density of synaptophysin puncta ($p<0.01$), there was no significant effect of the genotype ($p>0.45$) on synapse density. We also stained the cultures against GAD67, a specific marker for GABAergic neurons. A clear increase

in staining could be observed from DIV 12 to 18 to 21, without an obvious difference in the amount of GAD67 immunoreactivity between the two genotypes (Figure 5g-l).

5. Discussion

Networks formed by neurons differentiated from MeCP2-/y mES cells show clear functional deficits compared to wt cultures. We found small, but significant differences in voltage-gated potassium currents and in AP half-with and –frequency between genotypes. Both excitatory- and particularly inhibitory synaptic activity was significantly lower in MeCP2-/y compared to wt cultures. Both sEPSCs and sIPSCs appeared at the same age (DIV 11) in MeCP2-/y and wt cultures; and while we could not statistically resolve it, the deficit in synaptic activity appears larger at later compared to early developmental stages. We did not detect a significant difference in the synapse density between wt and MeCP2-/y cultures. A deficit in initial synapse formation or later in the number of synapses can therefore not explain the reduced synaptic activity.

Voltage-gated potassium currents are significantly stronger in young MeCP2-/y neurons compared to age-matched wt neurons; this is compatible with the shorter AP half-width that we observe in young MeCP2 deficient neurons. The AP frequency is significantly higher in MeCP2-/y cultures, however the effect is not stable over time. Since MeCP2-/y neurons actually show a higher propensity to spike and since the effects on synaptic activity are most pronounced at later developmental stages the lower synaptic activity is not simply a consequence of lower excitability in MeCP2-/y cultures.

Previous studies using ES and iPS cultures have found differences in the activity of voltage-sensitive sodium channels in cultures of MeCP2-/y neurons (Okabe, Kusaga et al. 2010) (Farra, Zhang et al. 2012). Such differences were not found in another study of cultured neurons (Marchetto, Carromeu et al. 2010). Interestingly we do not find a difference in I_{Na}, but in I_K between MeCP2-/y and wt cultures in our system. Several recent studies have looked at the impact of MeCP2 mutations on intrinsic excitability in different brain regions. In one study on locus coeruleus neurons, the authors found altered expression levels of several voltage-dependent conductances in MeCP2-/y mice compared to wt controls (Zhang, Cui et al. 2010). APs had a lower threshold, but were slightly prolonged in MeCP2-/y neurons; the overall effect of the loss of MeCP2 on neuronal excitability in this study depended somewhat on the cell type studied (Zhang, Cui et al. 2010). In other brain regions, such as the cortex, no

differences in intrinsic excitability were detected between MeCP2 deficient and wt mice (Dani, Chang et al. 2005). MeCP2 expression seems to affect neuronal excitability relatively mildly and in a cell-type dependent manner.

Several groups have studied synapse development and plasticiy in MeCP2 mutated mice (Nelson, Kavalali et al. 2006) (Chao, Zoghbi et al. 2007) (Dani and Nelson 2009) (Wood, Gray et al. 2009) (Zhang, Zak et al. 2010). In all of these studies, deficits in synaptic maturation either of excitatory, or inhibitory connections were found after a certain developmental delay. This indicates that deficits in connectivity after an initially normal period of synapse formation are a common finding in mouse models of RTT. A lack of fundamental deficits in neuronal excitability, paired with a deficit in synapse maturation is also compatible with RTT patient's symptoms, which occur after a phase of initially normal mental development. We now describe a variant of such a pathology in our mES cell derived neurons.

The molecular nature of the synaptic deficit has not yet been elucidated for any of the systems tested. The initially normal development and the different effects on either excitatory or inhibitory synaptic transmission in various brain regions argue against key elements of the synaptic release machinery to be affected. In some studies a reduced number of dendritic spines or of synapses was described (Fukuda, Itoh et al. 2005) (Smrt, Eaves-Egenes et al. 2007). While we found no difference in the overall density of presynaptic terminals, we cannot be sure that the exact distribution of terminals is the same in MeCP2-/y compared to wt cultures. Different studies have found different types of synapses to be affected by a lack of MeCP2, depending on the brain region studied (Noutel, Hong et al. 2011) (Durand, Patrizi et al. 2012). Alterations in cell adhesion molecules or scaffolding proteins with differential distributions in different brain regions could explain such findings.

mES cell-derived neuronal cultures can produce relatively homogeneous neuronal tissue with an essentially limitless supply. Transcriptome analysis of such tissue might yield candidate molecules responsible for the deficits we observe. Key elements of the known RTT pathology in early developing neural networks could be replicated in our system. This makes it a useful tool to further investigate functional deficits of MeCP2 deficient neurons and to study candidate interventions aimed at slowing or reversing the changes observed.

6. References

Amir, R. E., I. B. Van den Veyver, et al. (1999). "Rett syndrome is caused by mutations in X-linked MECP2, encoding methyl-CpG-binding protein 2." Nature genetics **23**(2): 185-188.

Barkus, C. (2013). "Genetic mouse models of depression." Current topics in behavioral neurosciences **14**: 55-78.

Baschong, W., M. Duerrenberger, et al. (1999). "Three-dimensional visualization of cytoskeleton by confocal laser scanning microscopy." Methods in enzymology **307**: 173-189.

Ben-Ari, Y. (2002). "Excitatory actions of gaba during development: the nature of the nurture." Nature reviews. Neuroscience **3**(9): 728-739.

Bibel, M., J. Richter, et al. (2007). "Generation of a defined and uniform population of CNS progenitors and neurons from mouse embryonic stem cells." Nature protocols **2**(5): 1034-1043.

Biella, G., F. Di Febo, et al. (2007). "Differentiating embryonic stem-derived neural stem cells show a maturation-dependent pattern of voltage-gated sodium current expression and graded action potentials." Neuroscience **149**(1): 38-52.

Chahrour, M. and H. Y. Zoghbi (2007). "The story of Rett syndrome: from clinic to neurobiology." Neuron **56**(3): 422-437.

Chang, Q., G. Khare, et al. (2006). "The disease progression of Mecp2 mutant mice is affected by the level of BDNF expression." Neuron **49**(3): 341-348.

Chao, H. T., H. Y. Zoghbi, et al. (2007). "MeCP2 controls excitatory synaptic strength by regulating glutamatergic synapse number." Neuron **56**(1): 58-65.

Chen, R. Z., S. Akbarian, et al. (2001). "Deficiency of methyl-CpG binding protein-2 in CNS neurons results in a Rett-like phenotype in mice." Nature genetics **27**(3): 327-331.

Dani, V. S., Q. Chang, et al. (2005). "Reduced cortical activity due to a shift in the balance between excitation and inhibition in a mouse model of Rett syndrome." Proceedings of the National Academy of Sciences of the United States of America **102**(35): 12560-12565.

Dani, V. S. and S. B. Nelson (2009). "Intact long-term potentiation but reduced connectivity between neocortical layer 5 pyramidal neurons in a mouse model of Rett syndrome." The Journal of neuroscience : the official journal of the Society for Neuroscience **29**(36): 11263-11270.

Dirkx, R., Jr., A. Thomas, et al. (1995). "Targeting of the 67-kDa isoform of glutamic acid decarboxylase to intracellular organelles is mediated by its interaction with the NH2-terminal region of the 65-kDa isoform of glutamic acid decarboxylase." The Journal of biological chemistry **270**(5): 2241-2246.

Durand, S., A. Patrizi, et al. (2012). "NMDA receptor regulation prevents regression of visual cortical function in the absence of Mecp2." Neuron **76**(6): 1078-1090.

Ebert, D. H. and M. E. Greenberg (2013). "Activity-dependent neuronal signalling and autism spectrum disorder." Nature **493**(7432): 327-337.

Farra, N., W. B. Zhang, et al. (2012). "Rett syndrome induced pluripotent stem cell-derived neurons reveal novel neurophysiological alterations." Molecular psychiatry **17**(12): 1261-1271.

Fukuda, T., M. Itoh, et al. (2005). "Delayed maturation of neuronal architecture and synaptogenesis in cerebral cortex of Mecp2-deficient mice." Journal of neuropathology and experimental neurology **64**(6): 537-544.

Gelman, D. M. and O. Marin (2010). "Generation of interneuron diversity in the mouse cerebral cortex." The European journal of neuroscience **31**(12): 2136-2141.

Guy, J., J. Gan, et al. (2007). "Reversal of neurological defects in a mouse model of Rett syndrome." Science **315**(5815): 1143-1147.

Guy, J., B. Hendrich, et al. (2001). "A mouse Mecp2-null mutation causes neurological symptoms that mimic Rett syndrome." Nature genetics **27**(3): 322-326.

Hagberg, B. and G. Hagberg (1997). "Rett syndrome: epidemiology and geographical variability." European child & adolescent psychiatry **6 Suppl 1**: 5-7.

Huang, Z. J., G. Di Cristo, et al. (2007). "Development of GABA innervation in the cerebral and cerebellar cortices." Nature reviews. Neuroscience **8**(9): 673-686.

Marchetto, M. C., C. Carromeu, et al. (2010). "A model for neural development and treatment of Rett syndrome using human induced pluripotent stem cells." Cell **143**(4): 527-539.

Moretti, P. and H. Y. Zoghbi (2006). "MeCP2 dysfunction in Rett syndrome and related disorders." Current opinion in genetics & development **16**(3): 276-281.

Nelson, E. D., E. T. Kavalali, et al. (2006). "MeCP2-dependent transcriptional repression regulates excitatory neurotransmission." Current biology : CB **16**(7): 710-716.

Nichols, J. and Q. L. Ying (2006). "Derivation and propagation of embryonic stem cells in serum- and feeder-free culture." Methods in molecular biology **329**: 91-98.

Nissenkorn, A., E. Gak, et al. (2010). "Epilepsy in Rett syndrome---the experience of a National Rett Center." Epilepsia **51**(7): 1252-1258.

Noutel, J., Y. K. Hong, et al. (2011). "Experience-dependent retinogeniculate synapse remodeling is abnormal in MeCP2-deficient mice." Neuron **70**(1): 35-42.

Okabe, Y., A. Kusaga, et al. (2010). "Neural development of methyl-CpG-binding protein 2 null embryonic stem cells: a system for studying Rett syndrome." Brain research **1360**: 17-27.

Okita, K. and S. Yamanaka (2011). "Induced pluripotent stem cells: opportunities and challenges." Philosophical transactions of the Royal Society of London. Series B, Biological sciences **366**(1575): 2198-2207.

Picken Bahrey, H. L. and W. J. Moody (2003). "Early development of voltage-gated ion currents and firing properties in neurons of the mouse cerebral cortex." Journal of neurophysiology **89**(4): 1761-1773.

Rett, A. (1966). "[On a unusual brain atrophy syndrome in hyperammonemia in childhood]." Wiener medizinische Wochenschrift **116**(37): 723-726.

Ribera, A. B. (1999). "Potassium currents in developing neurons." Annals of the New York Academy of Sciences **868**: 399-405.

Scharf, S. H. and M. V. Schmidt (2012). "Animal models of stress vulnerability and resilience in translational research." Current psychiatry reports **14**(2): 159-165.

Shahbazian, M., J. Young, et al. (2002). "Mice with truncated MeCP2 recapitulate many Rett syndrome features and display hyperacetylation of histone H3." Neuron **35**(2): 243-254.

Smrt, R. D., J. Eaves-Egenes, et al. (2007). "Mecp2 deficiency leads to delayed maturation and altered gene expression in hippocampal neurons." Neurobiology of disease **27**(1): 77-89.

Spitzer, N. C., A. Vincent, et al. (2000). "Differentiation of electrical excitability in motoneurons." Brain research bulletin **53**(5): 547-552.

Tamamaki, N., Y. Yanagawa, et al. (2003). "Green fluorescent protein expression and colocalization with calretinin, parvalbumin, and somatostatin in the GAD67-GFP knock-in mouse." The Journal of comparative neurology **467**(1): 60-79.

Wood, L., N. W. Gray, et al. (2009). "Synaptic circuit abnormalities of motor-frontal layer 2/3 pyramidal neurons in an RNA interference model of methyl-CpG-binding protein 2 deficiency." The Journal of neuroscience : the official journal of the Society for Neuroscience **29**(40): 12440-12448.

Zhang, X., N. Cui, et al. (2010). "Intrinsic membrane properties of locus coeruleus neurons in Mecp2-null mice." American journal of physiology. Cell physiology **298**(3): C635-646.

Zhang, Z. W., J. D. Zak, et al. (2010). "MeCP2 is required for normal development of GABAergic circuits in the thalamus." Journal of neurophysiology **103**(5): 2470-2481.

Zhou, Z., E. J. Hong, et al. (2006). "Brain-Specific Phosphorylation of MeCP2 Regulates Activity-Dependent Bdnf Transcription, Dendritic Growth, and Spine Maturation." Neuron **52**(2): 255-269.

Zoghbi, H. Y. (2003). "Postnatal neurodevelopmental disorders: meeting at the synapse?" Science **302**(5646): 826-830.

7. Figure Legend

Figure 1

mES cell-derived neurons show early maturation. a-c) DIC images of early neuronal differentiation in stem cell derived cultures. a) Image of embryoid bodies before dissociation; scale bar: 100 µm. Progenitor cells 6 h after plating b) and at DIV 1 c); scale bar: 20 µm. Immunostainings against doublecortin d), actin staining with phalloidin e). f) Overlay of doublecortin and phallodin stain with DAPI stain (blue) and the corresponding DIC image g) in wt cultures at DIV 3. h-k) The corresponding pictures from MeCP2-/y cultures. Scale bar: 20 µm. l-m) Early development of neuronal physiology; the numbers next to the traces indicate the respective resting membrane potential. l) Reaction of wt and MeCP2-/y neurons to negative (bottom traces) and positive (top traces) somatic current injections at DIV 3. m) Reaction of wt and MeCP2-/y neurons to positive somatic current injections.

Figure 2

Developmental characterization of voltage-gated sodium- and potassium currents. Sample traces and I-V curves for voltage activated inward sodium currents (red) and voltage activated outward potassium currents (black). Data points for the I-V curves plot peak inward current (red squares) against the holding potential after depolarization and the sustained outward current (black dots) against the holding potential after depolarization. a-d) Increase in voltage activated whole-cell currents from DIV 3 to DIV 21. e) Comparison of inward sodium current as a function of developmental age for wt (black) and MeCP2-/y (red) cultures. f) Comparison of outward potassium currents as a function of developmental age for wt (black) and MeCP2-/y (red) cultures.

Figure 3

Neuronal spiking patterns as a function of developmental age. Representative single spikes evoked by supra-threshold current injections in cultured neurons at a) DIV 6, b) DIV 12 and c) DIV 21. Repetitive spiking was evoked by current injections shown in Figure 1m. d-g) Analysis of the spiking parameters in wt (black) and MeCP2-/y (red) cultures as a function of time in culture. d) Data for the amplitude of the first AP, e) the half-width at half height for the first AP, f) the initial firing frequency and g) the frequency at the end of the train relative to the initial firing frequency.

Figure 4

Synaptic activity as a function of development. a-c) Traces of spontaneous activity in voltage-clamp. Top traces at -40 mV holding potential bottom traces at -60 mV respectively. d) Pharmacological characterization of synaptic currents. d1) Sample trace of one experiment with baseline recording a), after bath application of NBQX (10 µM) b) and bath application of picrotoxin (100 µM) c). d2) Inserts show the same regions as in d1) at higher temporal resolution. e) Frequency of sEPSCs as a function of time in culture for wt (black) and MeCP2-/y (red) cultures. f) Same data for sIPSCs.

Figure 5

Comparison of synaptic marker expression. Mature neurons from wt (a-c, g-i) and MeCP2-/y (d-f, j-l) were assessed immunocytochemically on DIV 12, DIV 18 and DIV 21 for expression of the presynaptic marker synaptophysin (a-f) and the marker of GABAergic neurons GAD-67 (g-l). Scale bar: 20 µm.

8. Figures

Figure 1

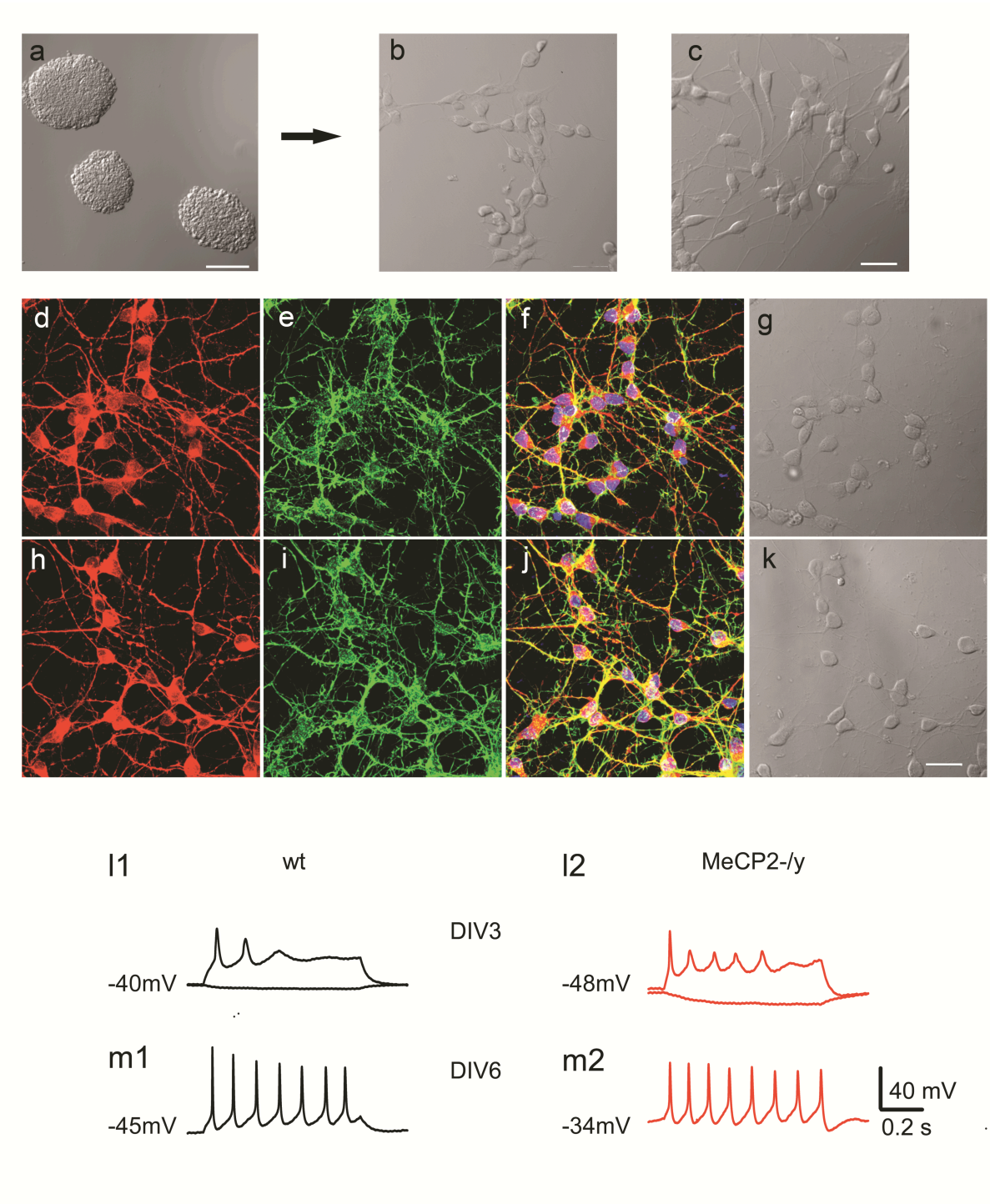

Figure 2

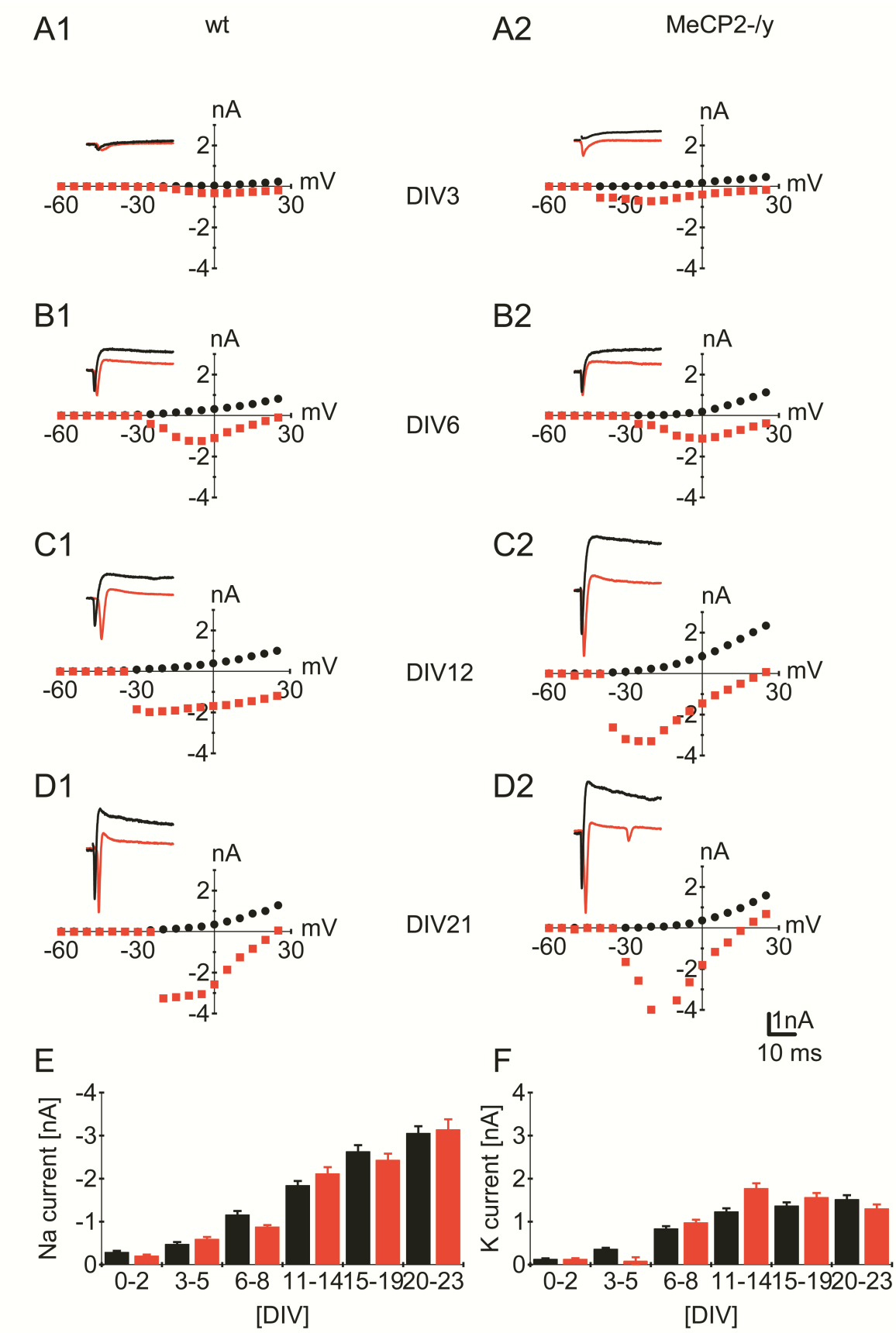
A1
wt
A2
MeCP2-/y
nA
mV
DIV3
B1
B2
DIV6
C1
C2
DIV12
D1
D2
DIV21
1nA
10 ms
E
F
Na current [nA]
K current [nA]
0-2
3-5
6-8
11-14
15-19
20-23
[DIV]

Figure 3

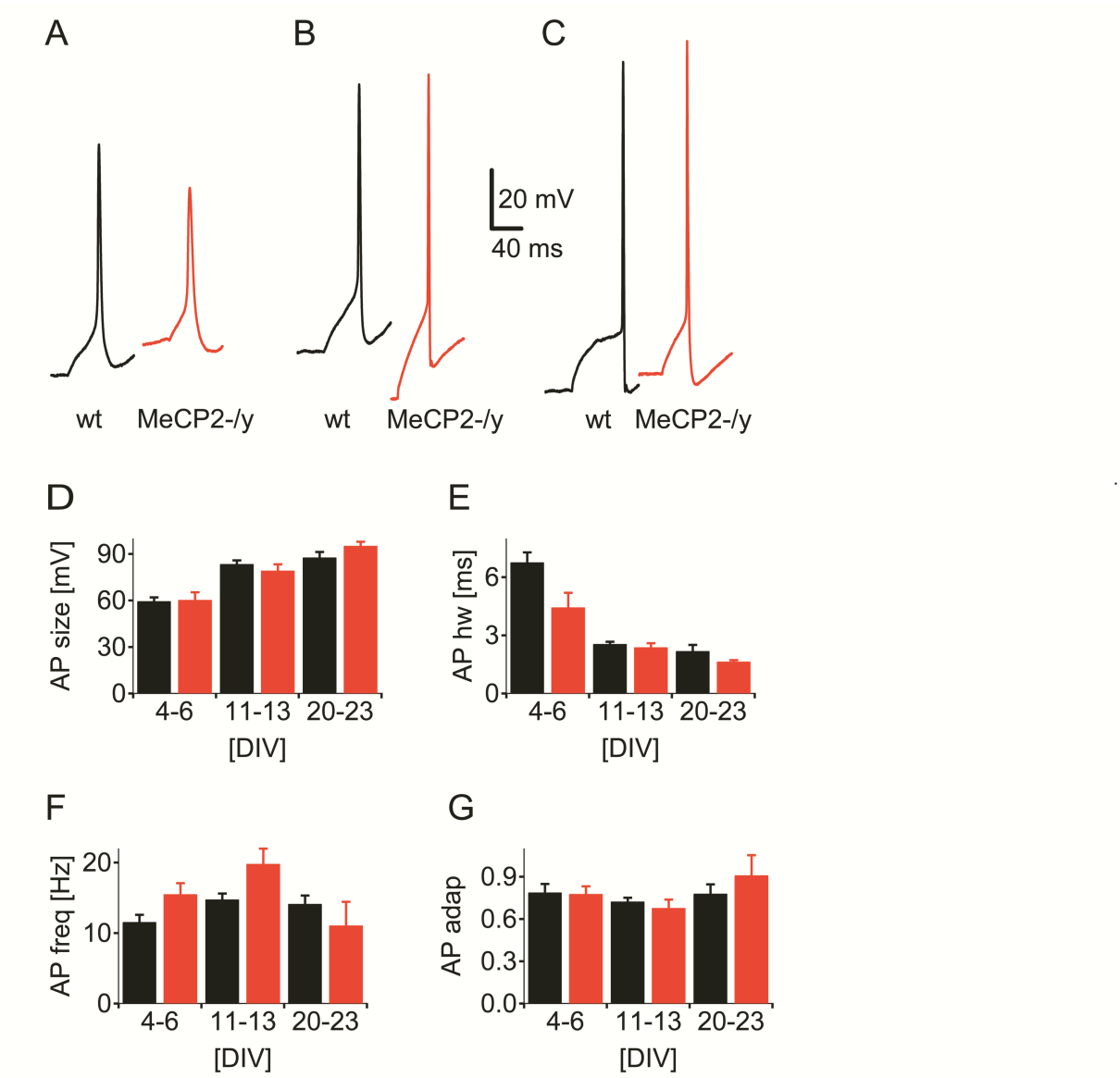
A
B
C
20 mV
40 ms
wt
MeCP2-/y
wt
MeCP2-/y
wt
MeCP2-/y
D
AP size [mV]
90
60
30
0
4-6
11-13
20-23
[DIV]
E
AP hw [ms]
6
3
0
4-6
11-13
20-23
[DIV]
F
AP freq [Hz]
20
10
0
4-6
11-13
20-23
[DIV]
G
AP adap
0.9
0.6
0.3
0.0
4-6
11-13
20-23
[DIV]

Figure 4

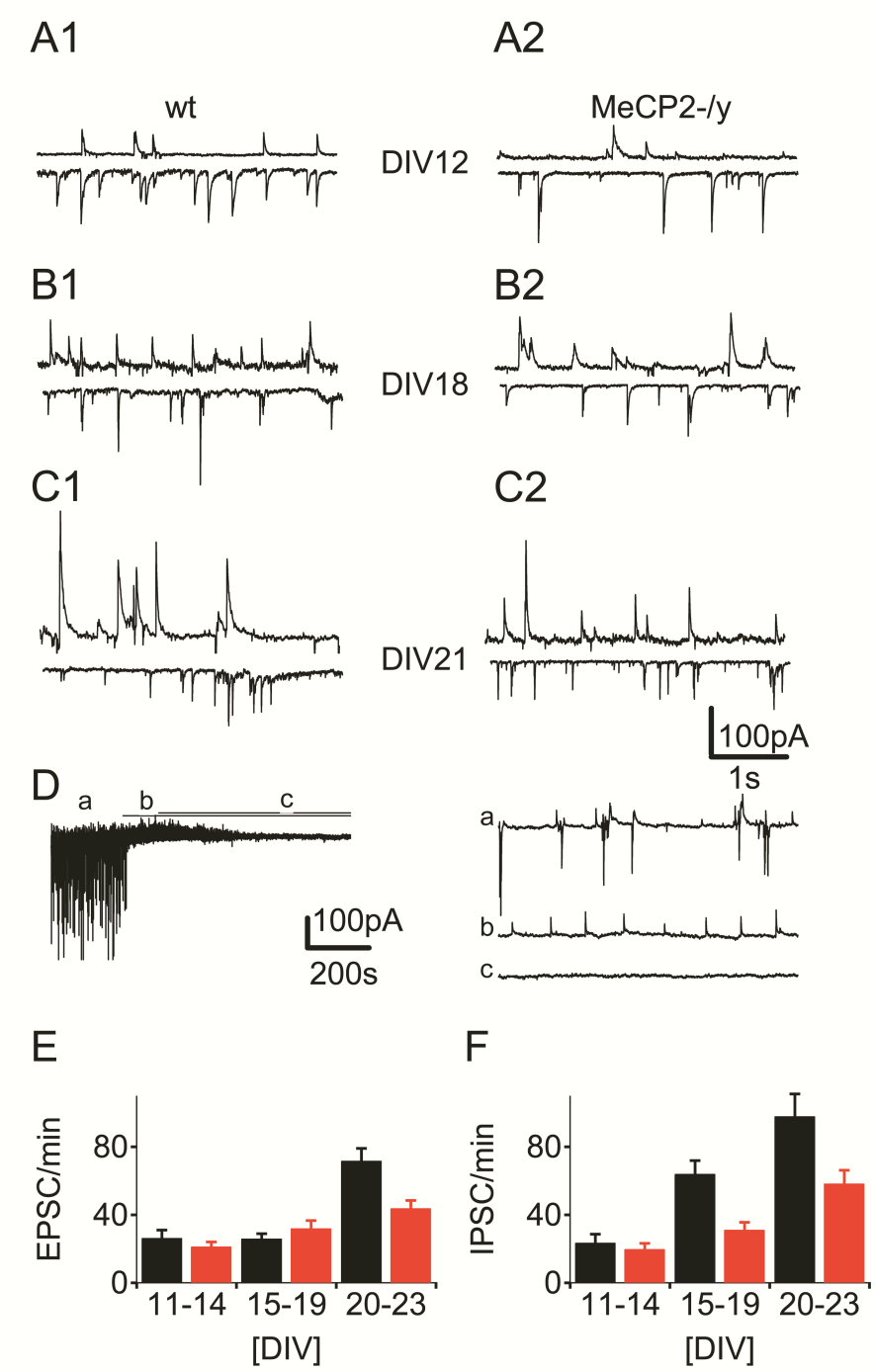
A1
A2
wt
MeCP2-/y
DIV12
B1
B2
DIV18
C1
C2
DIV21
100pA
1s
D
a
b
c
100pA
200s
a
b
c
E
F
EPSC/min
IPSC/min
80
40
0
11-14
15-19
20-23
[DIV]

Figure 5

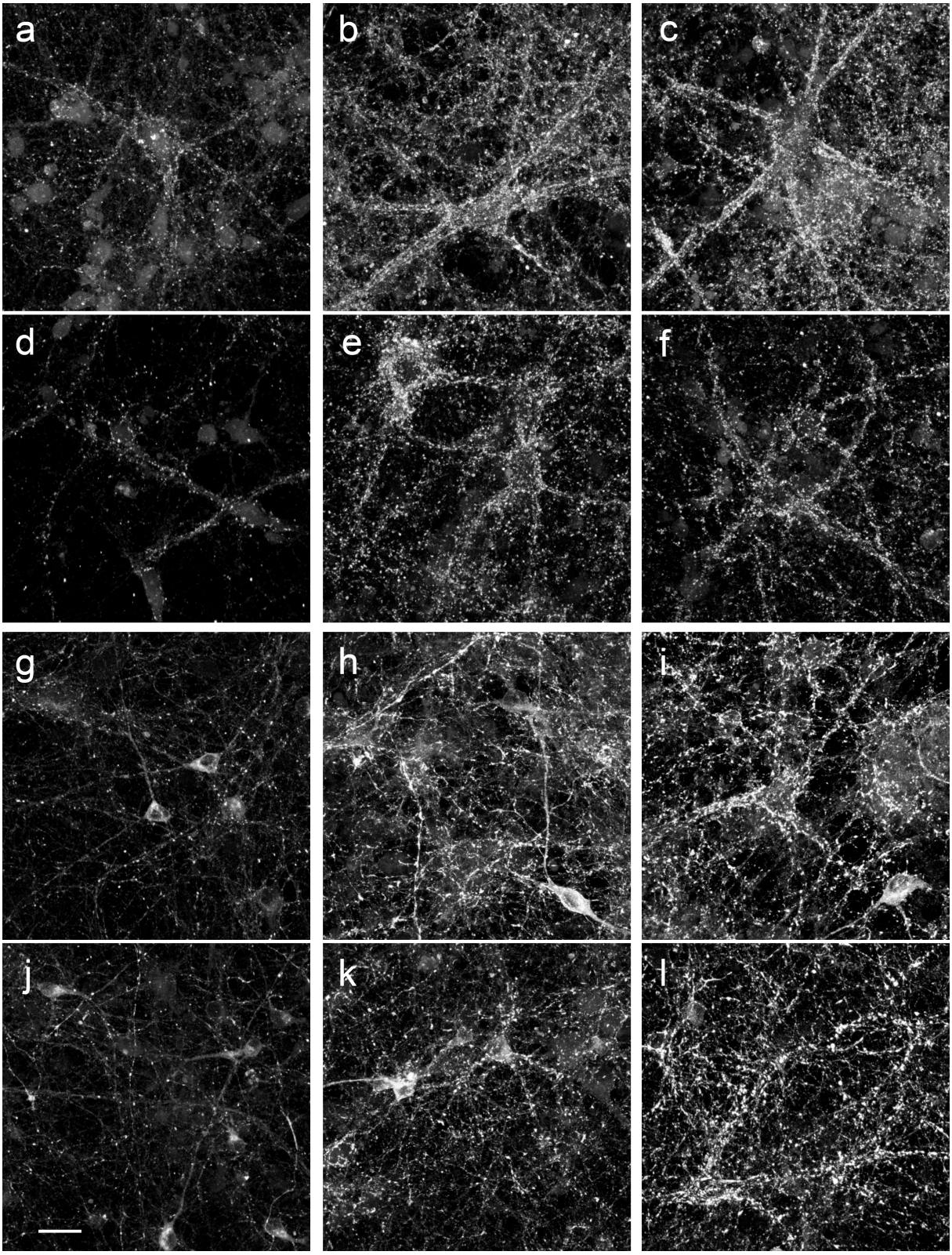

IV. Chapter 3

Interneurons in stem cell derived cultures

Lydia Barth[1] M.S., Rosmarie Sütterlin[1] and Kaspar Vogt[1*]

1
Neurobiology/Pharmacology
Biozentrum
University of Basel
Klingelbergstrasse 50/70
4056 Basel
Switzerland

1. Abstract

Functional neural networks need to maintain a balance between excitation and inhibition. We were interested in the establishment of such a balance in a highly reduced system in which we can maximally influence the conditions under which the network forms. Embryonic stem cell-derived neurons provide such a system. In these cultures precursor cells develop into neurons which form a dense network of synaptic connections. These networks contain around 20% interneurons, which dampen activity and prevent synchronized seizure-like events. We were investigating the functional development of all neurons and study the appearance of interneurons. Using a cell line which expresses GFP under the control of glutamic acid decarboxylase, 67 kDa isoform the main enzyme necessary for production of the inhibitory neurotransmitter GABA, we were able to determine that interneurons or their precursors appeared as soon as 24 hours after precursor plating.

We measured electrophysiological parameters such as voltage-gated channels and occurrence of action potentials to describe neuronal differentiation of the cells. In another series of experiments we were able to follow the fate of GFP-positive interneurons with a live-cell imaging system. By using pharmacology we wanted to find conditions under which larger or smaller numbers of interneurons than normal are generated.

2. Introduction

In vertebrate nervous systems two general classes of neurons can be distinguished: Those that release neurotransmitters leading to a depolarization and thus excitation of their target neurons and those that release transmitters dampening the activity of their target neurons. In the mammalian brain the most prevalent excitatory transmitter is glutamate, while the dominant inhibitory transmitter is gamma-aminobutyric acid (GABA). Most frequently GABA is released from neurons with typically a large number of short range connections within a network, therefore called interneurons. These inhibitory GABAergic interneurons provide a number of essential signalling functions, chief among them the control of the amount of excitation in the network. A loss of their function has been shown to underlie a number of neuropsychiatric disturbances from anxiety disorders to in extreme cases epileptic discharges 4 (Dani, Chang et al. 2005). A hyperfunction of the inhibitory system can also lead to an impaired function of the nervous system. In proper functioning neural networks therefore a finely tuned balance between excitatory and inhibitory activity therefore has to be established. This begins with the proper cell fate decision in immature neurons – of which on average about 20% will become GABAergic interneurons and 80% excitatory, mostly glutamatergic principal cells. In the mammalian forebrain interneurons develop from distinct pools of neural stem cells in the medial ganglionic eminence, from where they then migrate to their final position throughout the brain (Gelman and Marin 2010). While this scenario indicates that the niche in which the neurons develop determines their fate, other groups have postulated and provide evidence for a homeostatic mechanism controlling cell fate. In such a homeostatic system higher levels of excitatory activity would induce the creation of more GABAergic interneurons to maintain a stable signalling level. In frog spinal cords expression of (inhibitory) potassium channels was found to reduce the number of GABAergic neurons, while the overexpression of certain (excitatory) sodium channels increased the number of GABAergic interneurons (Spitzer, Vincent et al. 2000). For the forebrain no such data is available. In previous studies on murine embryonic stem (mES) cell derived neuronal cultures we have always found inhibitory synaptic activity and we were therefore wondering whether this system was suitable at addressing the genesis of GABAergic interneurons in a reduced and easily manipulated system.

We made use of mES cells derived from a mouse line which expresses the marker GFP under the control of the promoter of the main GABA producing enzyme, the 67 kD isoform of the glutamic acid decarboxylase (GAD67) (Tamamaki, Yanagawa et al. 2003). We studied the functional maturation of GAD67 mES cell-derived neuronal cultures, especially their synaptic activity. Cultures were subject to different growth conditions and the number of interneurons was assessed using GFP fluorescence.

3. Materials and methods

Cell culture and differentiation

Derivation of mES cells from GAD67-GFP knockin mice (Tamamaki, Yanagawa et al. 2003) on a C57/Bl6 background were carried out using an established protocol (Nichols and Ying 2006). mES derived from GAD67-GFP genotype were cultured and differentiated into neurons as described (Bibel, Richter et al. 2007). Briefly, after 4 days of embryoid body formation they are treated with 5 µM all-*trans*-retinoic acid (Sigma) for additional 4 days. Embryoid bodies are dissociated and neuronal precursors were plated on poly-L-ornithine (Sigma) /laminin (Roche) - coated glass cover slips (Assistent). At DIV 0 and 1 neuronal precursors were cultured in neural medium containing DMEM/F12, N-2 Supplement (100X) and penicillin/streptomycin and 1 mM glutamine (all Invitrogen). From DIV 2 the medium was changed to the differentiation medium containing Neurobasal medium, B-27 ® Supplement (50X), N-2 Supplement (100X), 0.6 mM glutamine and penicillin/streptomycin (all Invitrogen).

Electrophysiology

Cover slips with neurons were transferred to a bath chamber mounted to an inverse microscope (Axiovert 25, Carl Zeiss, Germany). Experiments were performed on DIV 0-8 and DIV 11-23 neurons in culture using a whole-cell voltage-clamp technique. Data were obtained using a Multiclamp 700A amplifier (Axon Instruments, USA). We used electrodes with an open tip resistance of 4-5 MΩ obtained by pulling borosilicate pipettes with 1.5 mm external diameter and 1.17 mm internal diameter without filament to a tip diameter of $\sim$1 *µ*m on a horizontal Puller (DMZ Puller, Zeitz GmbH, Germany). The intracellular solution was adapted to the culture medium the cells were cultivated in; for N2 medium it contained (mM): 110 K-D-gluconate, 5 KCl, 11 Tris-phosphocreatine, 1 EGTA, 4.5 MgATP, 10 HEPES, 0.3 Tris-GTP (pH 7.4 with KOH, 290 mOsm). The extracellular solution for cells coming from N2 medium used for DIV 0 and DIV 1 contained (in mM): 120 NaCl, 29 $NaHCO_3$, 4 KCl, 1 $CaCl_2$, 0.7 $MgCl_2$, 18 glucose, pH 7.4 when bubbled continuously with 95% O_2 and 5% CO_2. Intracellular solution for cultures coming from complete medium contained (mM): 100 K-D-gluconate, 5 NaCl, 1 EGTA, 5 MgATP, 10 HEPES, and 0.5 Tris-GTP (pH 7.4

with KOH, 210 mOsm). The extracellular solution for complete medium contained (in mM): 125 NaCl, 26 $NaHCO_3$, 1.25 $NaH_2PO_4*H_2O$, 2.5 KCl, 1.0 $MgSO_4$, 2.0 $CaCl_2$ and 11 glucose, pH 7.4 when bubbled continuously with 95% O_2 and 5% CO_2. Voltage-gated sodium- and potassium channels were detected in voltage- clamp mode at a holding potential of -60 mV. The holding potential was changed in a stepwise fashion from -75 mV to +25 mV in 5 mV increments and the voltage-gated peak inward current and maximal sustained outward current were measured. The inward currents were tetrodotoxin (TTX) sensitive, while the outward currents were blocked by tetraethyl-ammonium and 4-aminopyridine (TEA (3 mM) and 4-AP (1 mM)) (data not shown). Resting membrane potentials and action potentials were recorded in current-clamp mode. Somatic current injections were applied in 2.5 pA steps from -2.5 pA to +30 pA. Synaptic activity was measured in voltage-clamp mode: to detect spontaneous excitatory synaptic currents (sEPSCs) and spontaneous inhibitory synaptic currents (sIPSCs), cells were held at –60 mV. Responses were filtered at 5 kHz and digitized at 20 kHz. Recorded sEPSC and sIPSC were detected and analysed using Mini Analysis 6 (Synaptosoft, USA). All other data analysis was done with IGOR PRO 6.0 (Wavemetrics, USA) software. Two-way ANOVA were used for all statistical analysis (unless otherwise mentioned), with post hoc Bonferroni tests where indicated.

Immunocytochemistry and Imaging

Cells cultured on glass coverslips were rinsed twice with PBS pH 7.4 and fixed with 10% neutral buffered formalin (Sigma) for 20 min at room temperature (RT). After rinsing with PBS, coverslips were permeabilized for 5 min in 0.2% TritonX-100/PBS, rinsed with PBS and incubated for 1 h at RT in a humidified chamber with the following primary antibodies and dilutions (rb: rabbit, ms: mouse) : GFP (rb, 1:1000) glutamic acid decarboxylase, 67 kDa isoform, (GAD67) (ms, 1:500, Chemicon). After several washes with PBS, coverslips were incubated for 1 h with corresponding secondary antibodies: Cy3 (goat anti mouse IgG (H+L), 1:1000, Immuno Jackson), Cy5 (goat anti rabbit IgG (H+L), 1:300, Immuno Jackson). After several washes in PBS, coverslips were mounted in Mowiol-1188 as previously described(Baschong, Duerrenberger et al. 1999).

Confocal sections were recorded with a confocal laser scanning microscope Leica TCS SPE with DMI 4000B and processed with Imaris software and Adobe Photoshop version 10.0.

4. Results

We derived GAD67-GFP mES cells and differentiated these cells into neurons using established protocols (Tamamaki, Yanagawa et al. 2003) (Nichols and Ying 2006) (Bibel, Richter et al. 2007).

Progenitor cells showed already on DIV 0 a distinct, spindle shape morphology but no fluorescence (Figure 1 A). GFP fluorescence became visible at DIV 1 in 8 of 11 cultures (Figure 1 B). Over the course of the next few days in culture the intensity of the GFP label in the positive neurons increased (Figure 1 C&D) and 12/12 cultures contained distinct GFP positive cells by DIV 6 and 9. The number of detected cells per 500 by 500 µm field rose from 11 ± 4 to 21 ± 5 from DIV 1 to DIV 6 (N=8). We stained our cells with an antibody against GFP at DIV 5 and DIV 11 (Figure 2 B&F) to verify that the fluorescence observed in the unstained Cy2 channel stemmed from GFP expression. At the same time points direct antibody labeling was used to investigate the GAD67 expression patterns in the cultures (Figure 2 C&G).

We found a very good overlap of native GFP fluorescence and Cy3 labeled anti-GFP immunostaining in all living neurons (Figure 2 A&B and E&F). At later time points dying cells and dead material was found to show autofluorescence in the Cy2 channel (Figure 2 E&F). We could clearly detect GAD67 in the cultures already at early time points during development. In young cultures the labeling was weak and did not show a clear pattern (Figure 2 C), at DIV 11 the GAD67 signal showed a distinctly punctate staining, co-localizing with neural somata and processes (Figure 2 G). In the cell line used, GFP is produced instead of GAD67 in one allele (knock-in). While GFP can diffuse freely throughout the neuron, GAD67 shows the native distribution pattern, preferential labeling inhibitory presynaptic terminals (Dirkx, Thomas et al. 1995) (Figure 2 C&G).

All cells investigated showed voltage-activated rapid inward sodium- and slow outward potassium currents (Figure 1 E) and repetitive spiking upon somatic depolarization (Figure 1 F) at DIV 6. Both sodium- and potassium current amplitudes further increased until DIV 13 (Figure 2 I) and action potentials increased in amplitude and frequency and became faster (Figure 2 J). At DIV 13 spontaneous synaptic activity was observed in all cultures (Figure 2 K). Cells were held in voltage-clamp at -60 mV with a low-chloride internal solution. Inhibitory postsynaptic currents

(IPSCs) are seen as spontaneous outward currents (Figure 2 L) whereas excitatory postsynaptic currents (EPSCs) appear as spontaneous inward currents (Figure 2 M).

To test the influence of neural activity on the number of developing GABAergic neurons we compared GFP fluorescence at DIV 6 under standard culture conditions (Figure 3 A) with cultures grown for six days in the presence of 20 mM KCl (Figure 3 B) or the sodium channel blocker TTX (1 µM) (Figure 3 C). Neither depression of neuronal activity by TTX, nor depolarization of the neurons by KCl produced a visible change in the fluorescence observed (Figure 3 A-C). We measured the average somatic fluorescence intensity of GFP positive neurons in four randomly chosen 500 by 500 µm fields in two coverslips for each condition. We found no significant difference in the distribution of fluorescence intensities between control, KCl or TTX (Figure 3 D).

5. Discussion

In all the cultures a subset of mature neurons showed distinct GFP fluorescence in mature, synaptically active DIV 13 cultures. Above background fluorescence could clearly be detected in some DIV 1 cultures. The fluorescence intensity rose throughout the first days in culture and then leveled off. The number of cells increased as well. All cells investigated showed voltage-gated conductances, mature neuronal spiking patterns and synaptic activity by DIV 13. Using antibody staining against GFP and GAD67 we confirm that GFP fluorescence is a suitable marker for interneuron identity, as has been shown for this construct in (Tamamaki, Yanagawa et al. 2003). The number of GFP positive neurons and their intensity were not sensitive to manipulations aimed at changing neural activity. It would be interesting to know, whether the survival of interneurons in culture is controlled by neural activity. In-vivo interneurons are sensitive to the neurotrophic factor BDNF which is known to be released from primary neurons in an activity-dependent manner. Further experiments with older, synaptically active cultures will be necessary to test this hypothesis. In our system the generation of interneurons seems independent of neural activity. In fact the first signs of interneuronal cell fate decision occur at a time, when the neurons are very immature and barely active. In the time before network integration their survival does not depend on action potential generation. This seems to mimic the situation in the developing mammalian brain, where interneuron progenitors develop in niches remote from the location in which they will later function. The activity level in this niche would therefore not be relevant for their later signaling role. We do not yet know which factors are decisive for a given mES cell-derived neuron to become GABAergic. It is remarkable that in a culture system derived from an initially homogeneous population of mES cells a distinct subpopulation undergoes differentiation into GABAergic neurons. Inhibitory synaptic activity (as well as GAD67 expression) can be found as soon as the cultures form synaptically connected networks, thus these interneurons also functionally integrate.

In summary: We demonstrate a culture system in which the generation, survival and functional integration of GABAergic interneurons can be directly observed and which is easily amenable to genetic and pharmacologic manipulations. Similar to the situation in the mammalian brain, the initial generation of interneurons is not activity dependent.

6. References

Baschong, W., M. Duerrenberger, et al. (1999). "Three-dimensional visualization of cytoskeleton by confocal laser scanning microscopy." Methods in enzymology **307**: 173-189.

Ben-Ari, Y. (2002). "Excitatory actions of gaba during development: the nature of the nurture." Nature reviews. Neuroscience **3**(9): 728-739.

Bibel, M., J. Richter, et al. (2007). "Generation of a defined and uniform population of CNS progenitors and neurons from mouse embryonic stem cells." Nature protocols **2**(5): 1034-1043.

Dani, V. S., Q. Chang, et al. (2005). "Reduced cortical activity due to a shift in the balance between excitation and inhibition in a mouse model of Rett syndrome." Proceedings of the National Academy of Sciences of the United States of America **102**(35): 12560-12565.

Dirkx, R., Jr., A. Thomas, et al. (1995). "Targeting of the 67-kDa isoform of glutamic acid decarboxylase to intracellular organelles is mediated by its interaction with the NH2-terminal region of the 65-kDa isoform of glutamic acid decarboxylase." The Journal of biological chemistry **270**(5): 2241-2246.

Gelman, D. M. and O. Marin (2010). "Generation of interneuron diversity in the mouse cerebral cortex." The European journal of neuroscience **31**(12): 2136-2141.

Nichols, J. and Q. L. Ying (2006). "Derivation and propagation of embryonic stem cells in serum- and feeder-free culture." Methods in molecular biology **329**: 91-98.

Spitzer, N. C., A. Vincent, et al. (2000). "Differentiation of electrical excitability in motoneurons." Brain research bulletin **53**(5): 547-552.

Tamamaki, N., Y. Yanagawa, et al. (2003). "Green fluorescent protein expression and colocalization with calretinin, parvalbumin, and somatostatin in the GAD67-GFP knock-in mouse." The Journal of comparative neurology **467**(1): 60-79.

7. Figure Legend

Figure 1: Derivation of neurons from mouse embryonic stem cells

A-D) GFP antibody staining of early neuronal differentiation of GAD67- GFP stem cell derived cultures and bottom corresponding DIC with GFP positive neurons on DIV 0 (A), DIV 1 (B), DIV 3 (C) and DIV 6 (D). Scale bar: 30 µm. E-F) Early development of neuronal physiology on DIV 6; Sample traces and I-V curves for voltage activated inward sodium currents (red) and voltage activated outward potassium currents (black) (E). Data points for the I-V curves plot peak inward current (red squares) against the holding potential after depolarization and the sustained outward current (black dots) against the holding potential after depolarization. Reaction of GAD67-GFP neurons to positive somatic current injections at DIV 6 (F).

Figure 2:

Developmental characterization of GAD67-GFP stem cell derived cultures Morphology of interneurons at DIV 5 (A-D) and (E-H) on DIV 11: DIC with GFP positive neurons (A&E); GFP antibody staining (B&F); marker of GABAergic neurons GAD-67 (C&G) and the overlay of all (D&H). Scale bar: 30 µm. I-M) Mature neuronal physiology at DIV 13; Sample traces and I-V curves for voltage activated inward sodium currents (red) and voltage activated outward potassium currents (black) (1I). Data points for the I-V curves plot peak inward current (red squares) against the holding potential after depolarization and the sustained outward current (black dots) against the holding potential after depolarization. Repetitive spiking was evoked by supra-threshold current injections in cultured neurons at DIV 13 (J). Sample trace of spontaneous synaptic activity in voltage-clamp at -60 mV (K). Expanded view of sIPSC (L) and sEPSC (M) from sample trace (K) at higher temporal resolution.

Figure 3:

Pharmacological treatment of GAD67-GFP derived-neurons

A-B) Overlay of DIC and fluorescence image at DIV 6 of GAD67-GFP derived-neurons with GFP positive neurons in green; control condition (A), under treatment with KCl (B) and TTX (C); Scale bar: 30 µm. D) Cumulative histogram of green fluorescence intensity (arbitrary units) of neurons of cultures at DIV 6 under control condition and under treatment with KCl and TTX.

8. Figures

Figure 1

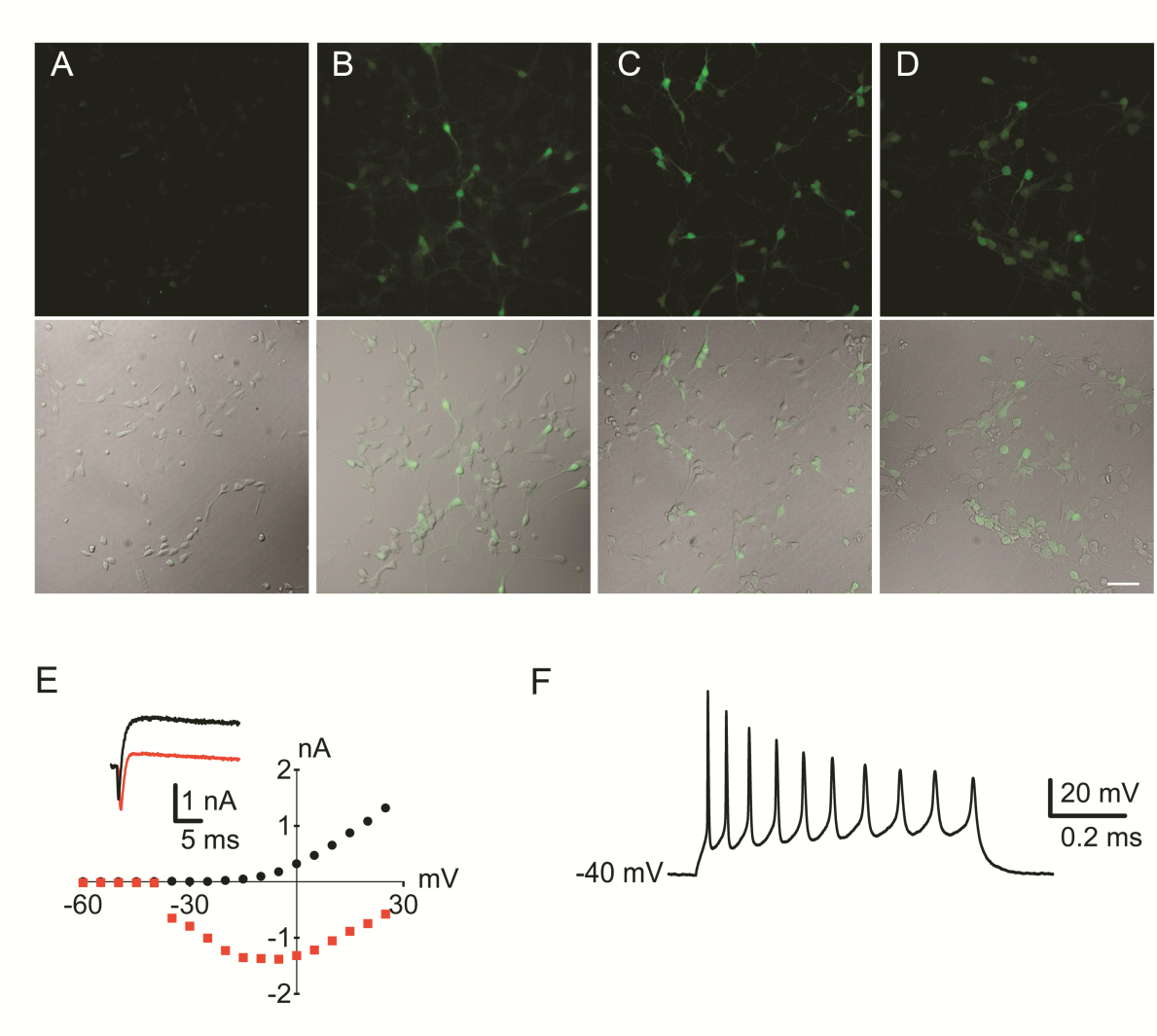

Figure 2

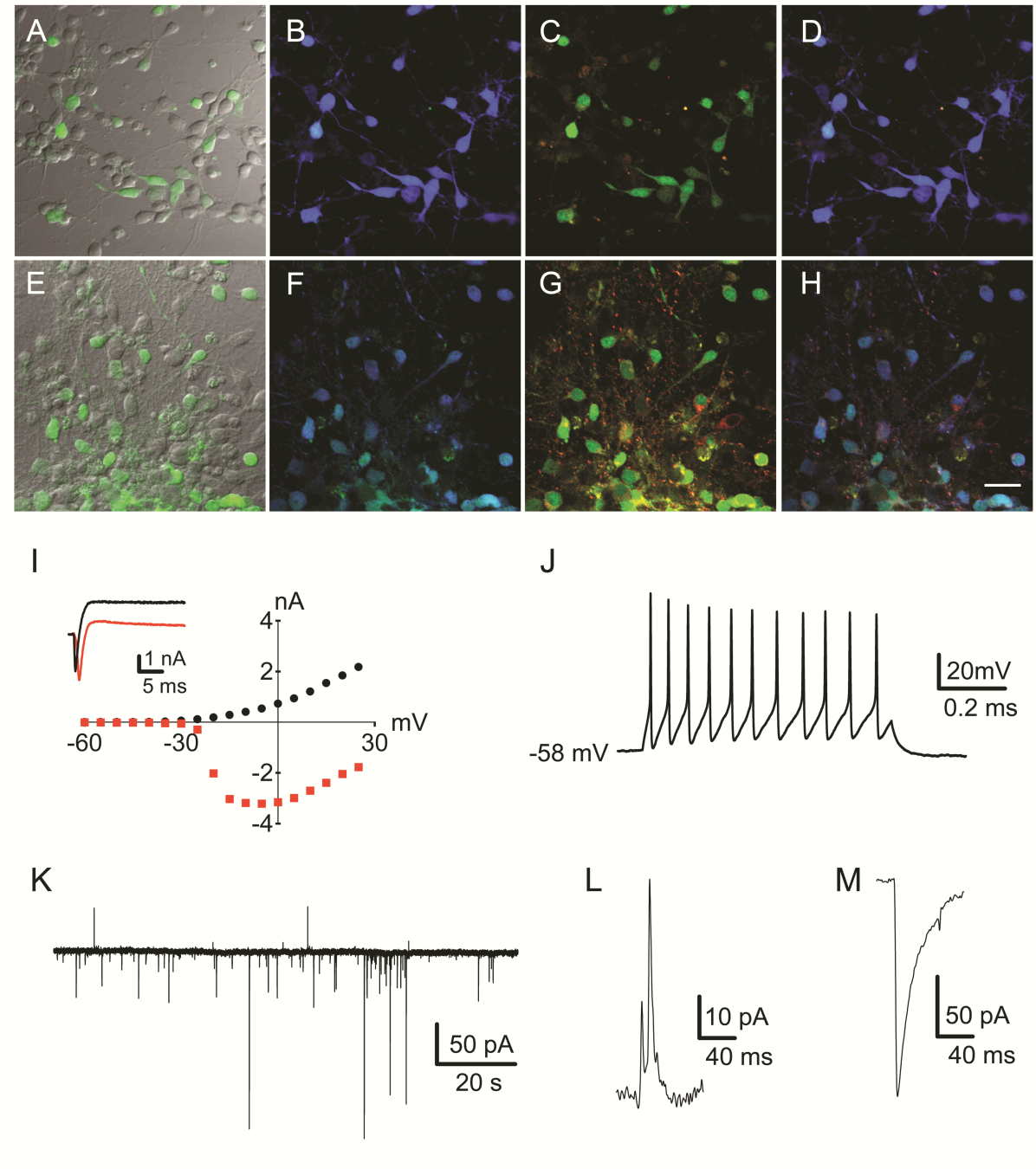
A
B
C
D
E
F
G
H
I
nA
4
2
-2
-4
1 nA
5 ms
-60
-30
30
mV
J
20mV
0.2 ms
-58 mV
K
50 pA
20 s
L
10 pA
40 ms
M
50 pA
40 ms

Figure 3

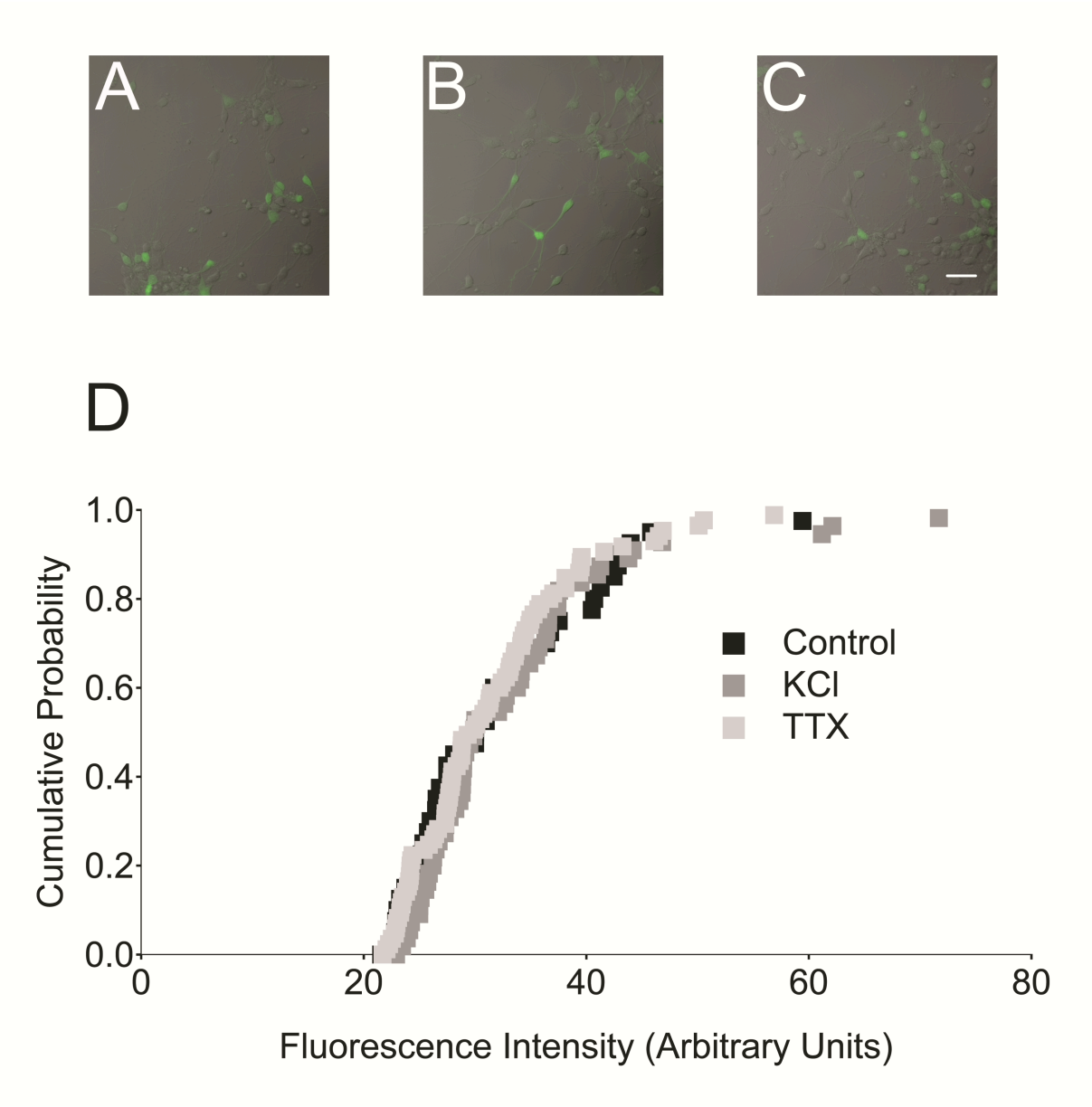
A
B
C
D
Cumulative Probability
1.0
0.8
0.6
0.4
0.2
0.0
0
20
40
60
80
Fluorescence Intensity (Arbitrary Units)
Control
KCl
TTX

V. Discussion

The successful differentiation of neurons in vitro from various mES cell backgrounds and genotypes permitted electrophysiological experiments with the goal to functionally characterize and better understand the development from immature to mature neurons.

The differentiation of reproducible and reliable mES cells is strongly depended on the quality of mES cells, as well as on the way they were cultured. Our cultures could be kept for up to 4 weeks in vitro with an optimal density and reliable function.

All our mES cell-derived cultures are not homogenous and contain more GABAergic neurons than previously published by other groups (Bibel, Richter et al. 2007). We observed various non-neuronal cells that are also found in primary cultures by using the actin staining phalloidin. Such cells might be relevant for a metabolic stability, or for the maturation and survival of neurons. Further investigations will be necessary to follow these hypotheses. The ratio between excitatory and inhibitory neurons was roughly 80:20 in all of our neuronal cultures, comparable to values found in in-vivo systems. Our analysis is based on 1654 measured cells from four different mouse strains, two of which also carry a genetic manipulation. The studies demonstrate for the first time that intrinsic membrane properties as RMP, voltage gated sodium- and potassium currents as well as maturation of action potentials show a different timing in the different backgrounds. This is also true for the maturation of the neural network. We found both an effect of the genetic background, as well as an effect of the MeCP2 mutation on the development of spontaneous synaptic activity. These differences strongly suggest that wild-type controls should be as closely related to the background strain of a genetically modified line as possible.

Finding the optimal recording conditions for the electrophysiology experiments was challenging. For example, after several trials we found the optimal condition for the electrophysiological extracellular solution for the N2 Medium. Especially the RMP depends heavily on the proper choice of extracellular solution. In the end, progenitors at DIV 0 and DIV 1 survived the recordings and showed the same results as tested under N2 medium conditions. We were surprised that precursor cells were stable already 6 h after plating and could be used for electrophysiological measurements - indicating that the plating process is not traumatic for the cells. The RMP is

hyperpolarized at around -57 mV for all tested wt genotypes while at DIV 2 they all depolarize to around -40 mV. Further experiments will be necessary to investigate the causes for this robust phenomenon. Interestingly, MeCP2 deficient cells and GAD67-GFP knock in cells show a more depolarized RMP of around -35 mV after plating. Again the reasons for this difference are unclear. Cells from all backgrounds and genotypes reliably hyperpolarize to -57 mV during their subsequent differentiation, indicating that these differences do not affect mature neurons. Recorded mES cells (data not shown, results from my Master thesis) already exhibit an RMP of -58 mV. The depolarized resting membrane potential of immature neurons during the second day of differentiation is therefore all the more surprising. It suggests that the cells transiently loose an important neuronal characteristic during the transition period and with the change to conditional medium. Gene-chip studies in the Barde lab (personal communication) indicate that the induction protocol initiates an early phase that is characterized by an enormous decrease of gene expression that covers many gene products. The beginning of neuron-specific gene expression is visible after approximately one day in vitro. It is tempting to speculate that the RMP of mES cells and immature neurons (DIV 0) is mediated by a set of channels that are later no longer produced and that the production of the channels mediating the mature RMP occurs with a delay. Further gene expression studies may shed light on this phenomenon.

We observe voltage-dependent inward sodium currents (I_{Na}) with fast activation and inactivation kinetics, as well as slow, non-inactivating outward potassium currents (I_K) during all stages of differentiation and in all tested genotypes. The presence of I_{Na} and I_K channels in very immature neurons is very interesting. It is possible that these channels were already expressed during embryoid body formation a stage during which we were not able to reliably patch cells, nevertheless the speed at which these channels appear suggests that they are a very early sign of neuronal differentiation. The I_{Na} and I_K currents are very low from DIV 0 – DIV 2. At this age the cells are much smaller and electrically tighter and are not able to fire action potentials either experimentally evoked or spontaneously occurring.

Due to increasing I_{Na} and I_K expression, action potentials were detected from DIV 3/DIV 4 in all studied genotypes. We performed a quantitative analysis of the functional neuronal maturation by measuring the size of the first AP in a train and its

half-width, as well as the initial frequency of APs in a train and their frequency adaptation.

Spontaneous excitatory (sEPSCs) and inhibitory (sIPSCs) postsynaptic currents appear at the same DIV in all cells, but we observe a different first occurrence of synaptic activity per se between the backgrounds. This appears to be different from the in-vivo situation, for which many groups have described the initial appearance of GABAergic synaptic activity, followed by a delayed formation of excitatory synaptic contacts.

Characterization of immature neuronal cultures using antibodies against doublecortin, phalloidin and DAPI show that by DIV 3 more than 90% of the cells in culture are immature neurons with a multipolar shape. With increasing age the cells tend to clump together - this has not only implications for their growth, but also for the further immunocytochemical analysis of the cultures. The culture conditions have to be kept strictly constant especially for the plating density to achieve reliable differentiation and therefore large fractions of neuronally differentiated cells. It turns out that the cultures have to have a special density in our case $750*10^5$ cells/24 well plate to see the same results by antibody staining and electrophysiological investigation specially for the development of synaptic activity.

Mature neurons can be characterized by using antibodies against MAP2, synaptophysin and GAD67. Stainings against the antibody MAP2 and synaptophysin indicate that in mES cell-derived neurons synapses are morphologically established already a few days before they become functional active. Synapse density could be measured by counting the number of synaptophysin positive puncta along MAP2-positive dendrites. The detection of interneurons by using the GAD67 antibody was observable at around DIV 11 but a reliable counting was impossible. Before that age a large number of cells expressed already low levels of the enzyme. This would indicate that the cells may decide at a later stage to either increase the expression levels and become full-fledged interneurons, or to decrease them substantially and thus change their cell fate to become excitatory neurons. For that reason we established a system in which a genetic marker expression replaced the antibody detection method.

We derived mES cells from GAD67-GFP mice and differentiated them into neurons. We confirmed by stainings against antibodies GFP and GAD67 that our green fluorescent neurons are GFP positive, GABAergic interneurons. We also tested whether the interneurons in culture reacted to TTX and KCl but we could not observe a clear activity dependent increase or decrease of GFP fluorescence.

We recently started using live cell imaging systems to observe the cell fate of excitatory and inhibitory neurons in vitro under different conditions. Unfortunately we spent too much time trying different systems and used many precursors until we found a reasonable system called Cell IQ. We could only perform two sets of experiments because of substantial problems in culturing the GAD67-GFP cells and the lack of availability of the Cell IQ machine, which is heavily booked out. Preliminary evidence shows that also in living unfixed cultures GFP fluorescence appears around 24 h after plating - as in our fixed stained culture. The GFP fluorescent signal appeared simultaneously in the majority of the cells that were later fluorescent. It would be interesting to study the reason for this surprising synchronicity. A small number of cells were observed in which the GFP signal disappeared after some time and then reappeared again. It is tempting to speculate that the cell fate decision can be reversed at least in some of these neurons. Unfortunately there was not enough time to analyse all experiments in sufficient detail to say more about the cell fate decision of interneurons.

VI. References

Ben-Ari, Y. (2002). "Excitatory actions of gaba during development: the nature of the nurture." Nature reviews. Neuroscience **3**(9): 728-739.

Bibel, M., J. Richter, et al. (2007). "Generation of a defined and uniform population of CNS progenitors and neurons from mouse embryonic stem cells." Nature protocols **2**(5): 1034-1043.

Ribera, A. B. (1999). "Potassium currents in developing neurons." Annals of the New York Academy of Sciences **868**: 399-405.

Spitzer, N. C., A. Vincent, et al. (2000). "Differentiation of electrical excitability in motoneurons." Brain research bulletin **53**(5): 547-552.

Okita, K. and S. Yamanaka (2011). "Induced pluripotent stem cells: opportunities and challenges." Philosophical transactions of the Royal Society of London. Series B, Biological sciences **366**(1575): 2198-2207.

VII. Acknowledgment

First of all I would like to thank Kaspar Vogt for the opportunity doing my phD thesis in his laboratory. He always provides assistance with help by theoretical questions, technical problems and giving the opportunity to present my data on congresses.

A great thank you to the group of the TMCF for providing me with a sterile hood and an incubator to carry out my cell culture. Special thanks to Liliane Todesco **f**or her friendly support and helping by cell culture problems.

Many thanks to Prof. Dr. Yves-Alain Barde and his group for giving me mES cells from E14Tg2a, MeCP2-/y, R1 and J1. Special to Morteza Yazdani and Vassiliki Nikoletopoulous who kindly taught me the differentiation protocol. I would like to thank Dr. Martijn Dekkers for scientific advice, critical discussions and helpful comments.

I would also like to thank my colleagues for the encouragement, helpful comments, ideas and the great team spirit. Especially to Rosi who did all the nice immune-stainings.
Special thanks to Silvia and Rosi for the morning coffees that significantly contributed to my work and made life in the lab fun…

Special thanks to my boyfriend, all my friends and my family for being there in both good times and in bad times.